Review

Alina D. Zamfir[1]
Laura Bindila[1]
Niels Lion[2]
Mark Allen[3]
Hubert H. Girault[2]
Jasna Peter-Katalinić[1]

[1]Institute for Medical Physics and Biophysics, University of Münster, Münster, Germany
[2]Laboratoire d'Electrochimie Physique et Analytique (LEPA), Ecole Polytechnique Fédérale de Lausanne (EPFL), Lausanne, Switzerland
[3]Advion BioSciences, Norwich, Norfolk, UK

Chip electrospray mass spectrometry for carbohydrate analysis

Currently two types of chip systems are used in conjunction with MS: out-of-plane devices, where hundreds of nozzles, nanospray emitters are integrated onto a single silicon substrate from which electrospray is established perpendicular to the substrate, and planar microchips, embedding a microchannel at the end of which electrospray is generated in-plane, on the edge of the microchip. In the last two years, carbohydrate research greatly benefited from the introduction and implementation of the chip-based MS. In two laboratories the advantages of the chip electrospray in terms of ionization efficiency, sensitivity, reproducibility, quality of data in combination with high mass accuracy, and resolution of detection were systematically explored for several carbohydrate classes: *O*- and *N*-glycopeptides, oligosaccharides, gangliosides and glycoprotein-derived *O*- and *N*-glycans, and glycopeptides. The current state-of-the-art in interfacing the chip electrospray devices to high-performance MS for carbohydrate analysis, and the particular requirements for method optimization in both positive and negative ion modes are reviewed here. The recent applications of these miniaturized devices and their general potential for glycomic-based surveys are highlighted.

Keywords: Chip electrospray ionization tandem mass spectrometry; Gangliosides; Glycans; Glycopeptides; Miniaturization; Protein glycosylation; Review DOI 10.1002/elps.200500101

Contents

Correspondence: Dr. Alina D. Zamfir, Institute for Medical Physics and Biophysics, University of Münster, Robert-Koch Strasse 31, D-48149 Münster, Germany
E-mail: zamfir@uni-muenster.de
Fax: +49-251-8355140

Abbreviations: AI, activated ion; **CDG**, congenital disorders of glycosylation; **dHex**, deoxyhexose; **ECD**, electron capture dissociation; **FTICR**, Fourier transform ion cyclotron resonance; **Fuc**, fucose; **Gal**, galactose; **GalNAc**, *N*-acetyl galactosamine; **GlcNAc**, *N*-acetyl glucosamine; **Glc**, glucose; **Hex**, hexose; **HexNAc**, *N*-acetyl hexosamine; **IgA1**, immunoglobulin A1; **IRMPD**, infrared multiphoton dissociation; **Neu5Ac**, *N*-acetyl neuraminic acid; ***O*-Ac**, *O*-acetylation; **QTOF**, quadrupole time-of-flight; **Ser**, serine; **SWIFT**, stored waveform inverse Fourier transform; **μTAS**, micro-total analysis systems; **Thr**, threonine; **TIC**, total ion chromatogram
For ganglioside abbreviations see Addendum.

1 Introduction

In the development of miniaturized microfluidic systems a significant progress in the past decade took place primarily due to numerous advantages of microchip analysis,

including the ability to analyze minute samples, the increased throughput and performance, as well as reduced costs. In addition, several laboratory procedures such as sample preparation, purification, separation, and detection have been integrated onto a single microchip unit forming the so-called micro-total analysis systems (μTAS) to allow enhancement in sensitivity, speed, and accuracy [1–4]. In the last years, by introducing MS as a detector, the potential and the applicability of μTAS have been significantly extended [5, 6]. On the other hand, the option for miniaturized, integrated devices for sample infusion into MS was driven by several technical, analytical, and economical advantages such as simplification of the laborious chemical and biochemical strategies required currently for MS research, minimization of sample handling and sample loss, elimination of possible cross-contamination, increased ionization efficiency, high quality of spectra, possibility for unattended high-throughput experiments, and the flexibility provided by the microchips for coupling to different MS configurations.

In the field of ESI–MS, two types of chip-based devices are currently being investigated. The first category is represented by the out-of-plane devices, where 100 or 400 nanospray emitters are integrated onto a single silicon substrate, from which electrospray is established perpendicular to the substrate [7]. These devices are amenable to high-throughput sample delivery to ESI-MS by automated infusion [8, 9] and have the potential to completely replace flow-injection analysis assays. Moreover, the technical quality of the nanosprayers obtained by advanced silicon microtechnology is so high, and the experiments so reproducible, that such devices have been found in some instances to give more robust and quantitative analyses than LC- or CE-MS and to be able to suppress the need for separation prior to MS analysis [10, 11].

Due to efficient ionization properties, silicon-based nanoESIchip/MS preferentially forms multiply charged ions, and the in-source fragmentation of labile groups attached to the main structural backbone is minimized, enhancing the sensitivity of the analysis.

The second category consists of planar or thin microchips, made from glass [12, 13] or polymer [14, 15] material, embedding a microchannel at the end of which electrospray is generated in-plane, on the edge of the microchip. During the last years, the progress in polymer-based microsprayer systems was promoted by development of simpler methods for accurate plastic replications and ease to create lower-cost disposable chips.

Though compatible to automation for high-throughput analysis, these designs are best suited to act like μTAS by integration of other analytical functions prior to sample delivery to the MS system, such as sample cleanup [16], analyte separation by CE [17], and chemical tagging [18]. Moreover, in comparison with glass nanospray capillaries, these thin microsprayers were found to provide superior stability of the spray with time, improved S/N at various flow rates.

Several approaches for interfacing MS to silicon, glass, or polymer chips, providing flow rates which include them in categories from nano- to microsprayers, were reported [19]. Different configurations such as single and triple quadrupole, TOF, IT, and ultrahigh-resolution Fourier-transform ion cyclotron resonance (FTICR) mass spectrometers were adapted to chip-based ESI and contributed significant benefits for various studies. However, as nicely illustrated already by a number of reviews [8, 11, 20–22] the general areas of implementation and applications of chip technologies either silicon-based, glass, or polymer microchips have by far been primarily genomics, drug discovery, and proteomics.

Carbohydrates are the most abundant class of organic components found in living organisms, characterized by a high degree of structural complexity. They are present in nature as either oligosaccharides or glycoconjugates in which the oligosaccharide portion is covalently linked to a protein and/or a lipid and occur ubiquitously displayed on macromolecules and the surface of cells. This biopolymer category is involved in basic biological functions, such as antigen recognition machinery, cellular adhesion of bacteria and viruses, and protein folding, stability, and trafficking [23]. Particular structures were found to represent biomarkers of severe diseases and others to play an essential role in fertilization and embryogenesis [24].

Despite the high biological importance of carbohydrates and the performance exhibited by chip-based MS methodologies, the glycomics field has benefited from the chip technology only to a limited extent. Optimization of ESI-chip/MS for operation in the negative ion mode to detect carbohydrate ions was considered a challenging task mostly due to the relative low ionization efficiency that ultimately leads to decreased sensitivity. Besides, each class of carbohydrates was shown to require particular and defined conditions for chip ionization followed by the MS detection. These conditions are strongly dependent on the type of the labile peripheral attachments on the sugar chain such as fucosylation, sialylation, sulfation, phosphorylation, the ionizability of the functional groups, the hydrophilic and/or hydrophobic nature, branching of the sugar chains *etc.* [25, 26].

However, during the past years, efforts have been invested toward implementation of chipESI-MS/MS in glycomics. Initial experiments for testing of general tech-

niques and methodology provided clear-cut evidence for high potential in applications of this technology to research projects requiring compositional and structural analysis of *N*- and *O*-glycans, *O*-glycopeptides, and gangliosides.

In this context, the purpose of a review highlighting the first achievements and trends in chip-based ESI-MS of carbohydrates is primarily to offer a general background for its better understanding and the motivations for such an analytical option. We believe that from this review the reader will learn the basic requirements for successful chip MS analysis of different carbohydrate categories and disclose the advantages of chip-based ESI-MS devices for their compositional and structural assays.

2 Thin chip polymer-based electrospray MS

2.1 Coupling of the thin chip microsprayer system to high-performance MS for carbohydrate analysis

For screening and sequencing of carbohydrates, recently, a disposable polymer microchip with integrated microchannels and electrodes was coupled to both a quadrupole TOF (QTOF) and an FTICR mass spectrometer [27, 28].

The chip presented in Fig. 1 was microfabricated by semiconductor techniques including photolithography [29]. For the microchip fabrication, the starting material was a polyimide foil of 75 μm thickness, which is coated on both sides with 5 μm copper. A photoresist was patterned on the copper-coated polyimide foil through a printed slide acting as a mask. Photoresist was then developed and chemical etching was used to remove the deprotected copper where microchannels are to be patterned. Polyimide was plasma-etched to the desired depth. As both sides of the substrate were exposed to the plasma, through-holes were fabricated to act as sample reservoirs and/or provide access to the microchannel.

The final microchannels were 120 μm wide, 45 μm deep (nearly "half moon" cross section), with 100 μm gold-coated microelectrodes placed at the bottom of the microchannel. A 35 μm polyethylene/polyethylene terephthalate was laminated to close the channels. As described by Gobry *et al.* [15], one end of each channel was manually cut in a tip shape, so that the outlet of the microchannel was located on the edge of the chip. For sample dispensing, either a reservoir was pasted over the inlet of the microchannel or the chip was sandwiched in a home-made chip holder with an integrated reservoir. For MS coupling one end of each channel was manually cut in a tip shape, which was visually inspected with a stereomicroscope. This way, the outlet of the microchannel is located on the edge of the chip, providing an in-plane electrospray.

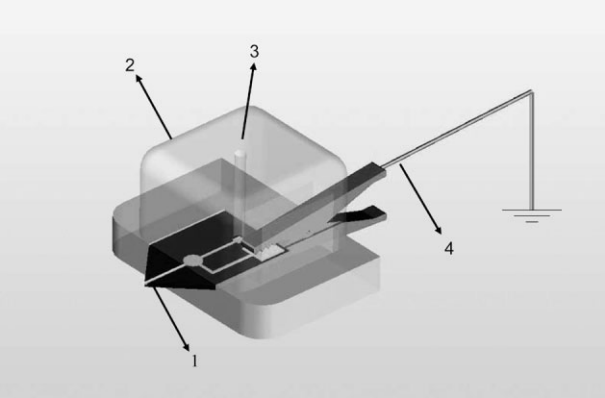

Figure 1. Schematic of the polymer chip holder with integrated reservoir. (1) Polymer chip; (2) sandwich chip holder; (3) sample reservoir; (4) conductive wire. Reproduced from [28]; with permission.

The thin polymer chip was coupled to a QTOF-MS (Micromass, UK) with Z-spray ion source geometry [27]. For sample loading, a microvial reservoir was pasted over the inlet-hole of the microchannel and the whole chip/reservoir assembly was mounted onto the mass spectrometer. An optimal coupling able to promote efficient ionization and sensitive detection of carbohydrates was found to require (i) stable electrical contact, (ii) careful positioning of the chip toward the MS sampling cone, (iii) adjustment of the ESI voltage and sampling cone voltages within 2–3 kV and 80–100 V, respectively, and (iv) systematic control of the solvent/analyte desolvation process. In order to realize the electrical contact to the ESI power supply, the ESI-QTOF sampler was removed and the chip system was directly connected to the ESI high-voltage plate, which is a fixed part of QTOF conventional ESI source. Exchange between the original source and chip system interface did not claim for any definitive dismantling or special mechanical modifications to either of the original assemblies and no further modifications on the QTOF-MS were reported as necessary. The position of chip emitter was adjusted in the vicinity of the entrance hole at a distance of about 5 mm from the QTOF-MS sampling cone. The ESI field was established by applying a voltage (2–3 kV) on the microchip electrode and an attractive potential (100–150 V) on the MS counter-electrode (cone). The voltage on the microelectrode was applied by using a conductive wire with one terminal connected to the chip electrode and the other fixed on the ESI high-voltage plate of the QTOF-MS instrument. Under

the formed high electric field, the fluid was electrokinetically driven through the chip microchannel from its inlet-hole toward the outlet-edge where the electrospray process occurred [27]. In the case of QTOF-MS, the ESI source is configured in *Z* geometry by the orthogonal alignment of the sampling capillary and MS counterelectrode.

In Fig. 2, a photography of the QTOF source assembly with mounted polymer chip is presented. The photography has been taken during the thin chipESI-QTOF-MS running, immediately after application of the negative voltages on both chip and counterelectrode. The ESI plume is clearly visible demonstrating the instant initiation of the electrospray. Under the same ESI-QTOF-MS conditions, the reported [27] in-run reproducibility in terms of sensitivity, spray stability, number of detected components/fragments, ion intensity, and charge state was almost 100%, while the day-to-day reproducibility was 95–100%.

The first interfacing of chip electrospray to FTICR-MS was reported in 2003 by Rossier *et al.* [30]. The system described by the authors included the thin polymer microchip placed into a specially designed holder and a 7 T FTICR MS (Bruker Daltonics) operating in the positive ion mode. In this study, the first application of the chip-FTICR system to proteome analysis and in particular to complex tryptic peptide mixture of the human microtubule-associated tau protein, considered as a target in neurofibrillary tangles characteristic of Alzheimer disease, is described. In the (+)chipESI-FTICR mass spectrum the primary structure including 18 serine (Ser) and threonine (Thr) phosphorylations could be directly identified, which clearly demonstrated the high analytical performance of the chipESI-FTICR-MS in proteomics.

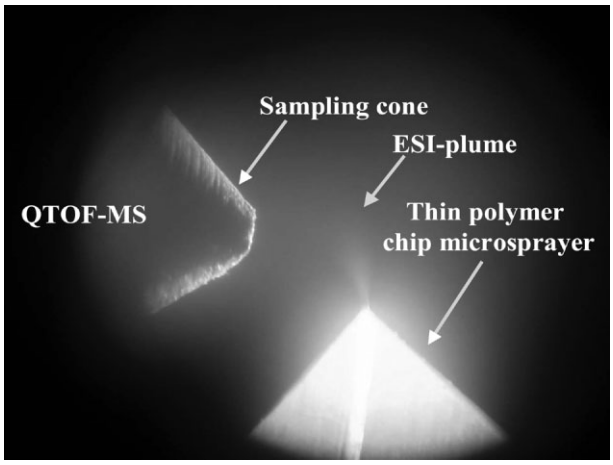

Figure 2. Photography of the thin polymer chip/ESI-QTOF-MS coupling, taken immediately after the application of the ESI voltages. Reproduced by permission of The Royal Society of Chemistry [27].

Last year, an Apex II FTICR mass spectrometer equipped with a 9.4 T superconducting actively shielded magnet and an Apex II Apollo ESI ion source was interfaced to the disposable thin polymer microchip, and the system was for the first time optimized in the negative ion mode and introduced in glycomics [28]. For sample loading and FTICR interfacing, the chip was sandwiched in a home-made chip holder with an integrated reservoir (Fig. 1) and positioned into the holder with the microchannel in contact with the reservoir and the front part extruding a few millimeters. Unlike the case of ESI-QTOF source, in the FTICR Apex II Apollo system the sampling capillary is grounded and the electric field is created by applying the ESI voltage on the MS metal-coated glass capillary. Therefore, for polymer chip interfacing to FTICR-MS, the chip was grounded *via* a conductive wire connected to the terminal gold-coated electrode. Another peculiarity of the FTICR ESI source is its direct spray geometry as a result of axial alignment of the sampling capillary and MS entrance. The microchip system was coupled to this ion source by an in-laboratory constructed mounting system consisting of a metal plate connected to the source by two 90° brackets. The in-house made mounting system was described as a robust and viable interfacing of the polymer chip to the FTICR-MS instrument.

2.2 Applications

2.2.1 Complex biological mixtures of glycopeptides

In human urine, carbohydrates are catabolic products excreted as either oligosaccharides or glycopeptides and their concentration, amount, and structure are known to vary under different physiological and/or pathological conditions. For this reason, monitoring the glycopeptide expression in human urine by MS could potentially become a method of diagnostic importance [31]. Various glycoconjugate pools extracted and purified from normal human urine and urine of patients suffering from diseases caused by aberrant glycosylation were already submitted to a number of MS-based analytical experiments to assess their potential for glycoscreening [32–35].

The thin chip microsprayer/QTOF-MS coupling described above was optimized in the negative ion mode for determination of *O*-GalNAc-Ser/Thr expression in the normal human urine [27]. A mixture of *O*-GalNAc glycosylated amino acids and peptides was dissolved in pure methanol to a concentration of 5 pmol/μL and an aliquot of 10 μL was dispensed into the reservoir pasted over the inlet of the chip microchannel. The negative ion mode electrospray process was initiated at 2.8 kV ESI voltage and 100 V potential of the sampling cone. At these values of

source parameters a constant and stable spray accompanied by a high intensity of the total ion current was generated. The signal was acquired over 20 scans (40 s) which, at the flow rate of about 200 nL/min provided by the microchip under these conditions, was equivalent to a sample consumption of 0.66 pmol. The spectrum combined over 20 scans exhibited a high S/N and a number of 26 different saccharide components. Fifteen species detected as singly and/or doubly charged ions expressed *O*-GalNAc-Ser/Thr core-motif extended by either sialylation or fucosylation. The mixture was found to be dominated by Ser- and Thr-linked disialo saccharides with chain lengths ranging from tetra- to octasaccharide. Interestingly, two new structures which could originate from glycopeptides with extended and further modified chains, not detectable before by any MS-related methods, were detected as doubly charged ions.

In order to test the limit of the microchip sensitivity for glycoconjugate detection, the solution was further diluted in pure methanol yielding an aliquot at 1.25 pmol/μL concentration. The signal was acquired over 20 scans, which was equivalent to 0.16 pmol sample consumption for this experiment. Even under these restrictive concentration conditions, a fair S/N was reported and 13 different components in the mixture could be still identified. All microchip spectra exhibited an interesting peculiarity related to ionic charge-state distribution. Thus, it was found that at 100 V cone potential, the charge distribution was not shifted toward lower values as observed in the capillary-based ESI-QTOF-MS experiments and the intensity of the signals corresponding to the doubly charged ions was still the highest ones. Moreover, the advantage of the microchip ESI-MS regarding the minimization of the in-source decay of the labile attachments such as *N*-acetyl neuraminic acid (Neu5Ac) was observed.

To investigate the possibility of rapid and accurate glycopeptide sequencing by MS/MS using the polymer chip for sample infusion, a doubly charged ion at *m/z* 532.08, assigned according to the *m/z* value to the already known structure of $NeuAc_2HexHexNAc$-Thr (Hex = hexose, HexNAc = *N*-acetyl hexosamine), was isolated and submitted to low-energy CID (−)microchip ESI-QTOF-MS/MS. Ion acceleration energy, collision gas pressure, and precursor ion isolation parameters were carefully adjusted to provide the full set of structural information upon the molecule. The product ion spectrum (Fig. 3) was obtained after 30 scans (1 min) of signal acquisition under the sample consumption of 1.23 pmol. A high S/N and significant number of diagnostic elements valuable for assessing the sialylation pattern and linkages specific to the core 1 type of *O*-glycosylated molecules were obtained.

In another study, the combination of the thin chip microsprayer performances with high accuracy and resolution of the FTICR-MS was designed and implemented for the screening in negative ion mode of several urine glyco-

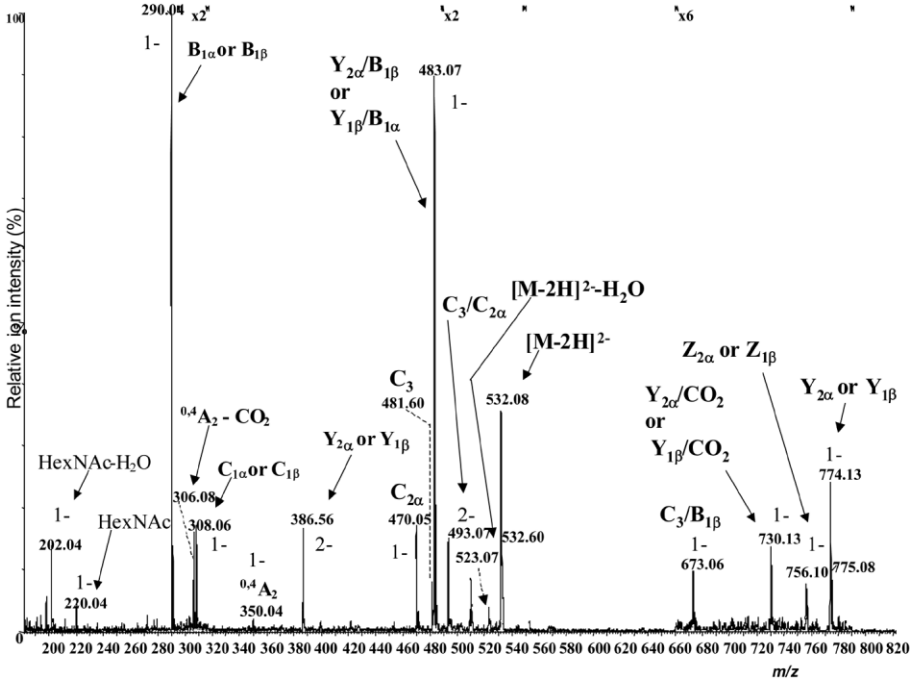

Figure 3. Microchip ESI/QTOF MS/MS of the $Neu5Ac_2Hex$-HexNAc-Ser doubly charged ion at *m/z* 532.08. ESI voltage: 2.8 kV; sampling cone potential: 100 V; solvent: methanol; average sample concentration: 5 pmol/μL; collision energy: 40 eV; signal acquisition: 30 scans; average sample consumption: 1.23 pmol. Nomenclature for assignment of fragment ions is according to [61, 62]. Reproduced by permission of The Royal Society of Chemistry [27].

peptide mixtures [28]. Special considerations of the thin chipESI/FTICR-MS parameters with respect to the direct spray configuration of the FTICR instrument were necessary here. The initiation of the electrospray was achieved at 1500–2500 V applied to the transfer capillary, while the fine positioning of the microsprayer toward the MS inlet turned out to be crucial for efficient transfer of the ionic species into the MS and long-term stability of the electrospray. The system was tested for compositional mapping of a mixture of *O*-glycosylated amino acids and peptides extracted and purified from urine of a patient suffering from Schindler disease and an age-matched healthy individual for comparative assay [28]. Schindler disease is a rare inherited metabolic disorder characterized by a deficiency of the lysosomal enzyme α-*N*-acetylgalactosaminidase (NAGA), which leads to an abnormal accumulation of sialylated and asialo-glycopeptides and oligosaccharides with α-*N*-acetylgalactosaminyl residues. The deficient NAGA is causing not only a 100 times higher concentration of *O*-glycans in patient urine than in healthy controls, but it was also found to give rise to unspecifically cleaved products consisting of longer saccharide chains [31, 36–38].

In Fig. 4, the (−)thin chipESI/FTICR mass spectrum of the *O*-glycosylated amino acids and peptides disease is depicted. After 50 scans of signal recording under a flow rate of approximately 200 nL/min, 27 ionic species could be already identified and straightforwardly assigned with an average mass accuracy of 5.41 ppm and a maximum sensitivity of 3 pmol/μL (Fig. 4). In comparison with the chipESI/FTICR spectrum of the normal urine glycopeptides, a higher content of pentasaccharides was observed, as documented by the doubly charged ion at *m/z* 562.193 and the corresponding singly charged ion at *m/z* 1125.386, assigned to Neu5AcHex$_2$HexNAc$_2$-Ser. The doubly charged ion at *m/z* 569.199 along with its singly charged counterpart at *m/z* 1139.401 was assigned to the homologous structure, Neu5AcHex$_2$HexNAc$_2$-Thr. Additionally, the hexasaccharides linked to Ser and Thr bearing two sialic acid moieties were detected at higher abundance than in the glycopeptide mixture from normal urine, and a nonasaccharide bearing three sialic acid moieties was for the first time detected at appreciable abundance as a doubly charged ion at *m/z* 1058.354 and assigned to the sodiated dehydrated Neu5Ac$_3$Hex$_2$HexNAc$_4$Ser with a mass accuracy of 4.6 ppm.

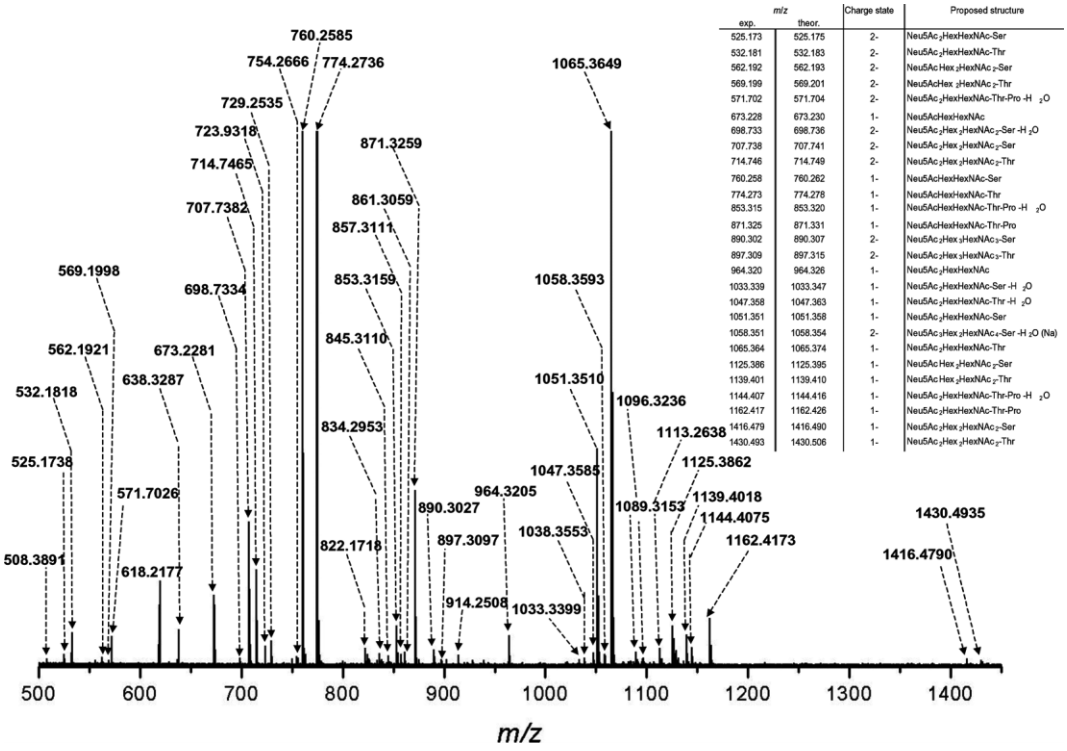

m/z exp.	m/z theor.	Charge state	Proposed structure
525.173	525.175	2-	Neu5Ac$_2$HexHexNAc-Ser
532.181	532.183	2-	Neu5Ac$_2$HexHexNAc-Thr
562.192	562.193	2-	Neu5AcHex$_2$HexNAc$_2$-Ser
569.199	569.201	2-	Neu5AcHex$_2$HexNAc$_2$-Thr
571.702	571.704	2-	Neu5Ac$_2$HexHexNAc-Thr-Pro -H$_2$O
673.228	673.230	1-	Neu5AcHexHexNAc
698.733	698.736	2-	Neu5Ac$_2$Hex$_2$HexNAc$_2$-Ser -H$_2$O
707.738	707.741	2-	Neu5Ac$_2$Hex$_2$HexNAc$_2$-Ser
714.746	714.749	2-	Neu5Ac$_2$Hex$_2$HexNAc$_2$-Thr
760.258	760.262	1-	Neu5AcHexHexNAc-Ser
774.273	774.278	1-	Neu5AcHexHexNAc-Thr
853.315	853.320	1-	Neu5AcHexHexNAc-Thr-Pro -H$_2$O
871.325	871.331	1-	Neu5AcHexHexNAc-Thr-Pro
890.302	890.307	2-	Neu5Ac$_2$Hex$_3$HexNAc$_3$-Ser
897.309	897.315	2-	Neu5Ac$_2$Hex$_3$HexNAc$_3$-Thr
964.320	964.326	1-	Neu5Ac$_2$HexHexNAc
1033.339	1033.347	1-	Neu5Ac$_2$HexHexNAc-Ser -H$_2$O
1047.358	1047.363	1-	Neu5Ac$_2$HexHexNAc-Thr -H$_2$O
1051.351	1051.358	1-	Neu5Ac$_2$HexHexNAc-Ser
1058.351	1058.354	2-	Neu5Ac$_3$Hex$_2$HexNAc$_4$-Ser -H$_2$O (Na)
1065.364	1065.374	1-	Neu5Ac$_2$HexHexNAc-Thr
1125.386	1125.395	1-	Neu5AcHex$_2$HexNAc$_2$-Ser
1139.401	1139.410	1-	Neu5AcHex$_2$HexNAc$_2$-Thr
1144.407	1144.416	1-	Neu5Ac$_2$HexHexNAc-Thr-Pro -H$_2$O
1162.417	1162.426	1-	Neu5Ac$_2$HexHexNAc-Thr-Pro
1416.479	1416.490	1-	Neu5Ac$_2$Hex$_2$HexNAc$_2$-Ser
1430.493	1430.506	1-	Neu5Ac$_2$Hex$_2$HexNAc$_2$-Thr

Figure 4. (−)Microchip ESI/FTICR MS of a fraction of *O*-glycosylated peptides extracted from urine of a patient diagnosed with Schindler disease. ESI voltage: 1.5–2.5 kV. Capillary exit: –79 V. Average sample concentration: 20 pmol/μL in methanol. Number of scans: 50. Average sample consumption: 2 pmol. Inset: table with assignment of the ions detected in the mixture by microchip ESI/FTICR-MS in the negative ion mode. Reproduced and adapted with permission from [28].

2.2.2 Gangliosides

Gangliosides are glycosphingolipids (GSLs) consisting of a mono- to polysialylated oligosaccharide chain of different lengths attached to a ceramide portion of variable composition with respect to the type of sphingoid base and fatty acid residues. They are abundant components of the central nervous system and their compositions undergo changes during brain development, maturation, aging, and neurodegeneration processes [39–41]. For these reasons, gangliosides are considered as tissue stage or diagnostic markers and potentially therapeutic agents. In human brain, region-specific differences in ganglioside composition and quantity, as well as in their distribution and expression have been demonstrated primarily by TLC, immunochemical, and immunohistochemical methods besides FAB-MS [42, 43] and capillary-based electrospray [44]. In all ESI-MS-related studies using either QTOF-MS [44], off-line CE/QTOF-MS, or FTICR-MS [45, 46], requirements for elevated values of ionization parameters and an extended time for CID-MS/MS signal acquisition, implying more sample consumption for identification and structural elucidation, were defined.

To explore the performance of the microchip ESI/QTOF-MS approach and the detection limits for structural characterization of gangliosides, a fraction of polysialylated gangliosides (GT1), isolated from the total native ganglioside mixture of normal adult human brain, was considered. For (−)microchip ESI/QTOF-MS analysis, GT1 sample was dissolved in pure methanol to a concentration of 5 pmol/μL and an aliquot of 10 μL was loaded into the microchip reservoir. To optimize the ionic current value, the (−)ESI voltage and cone potential were increased following a ramping procedure. The total ion chromatogram (TIC) profile indicated a maximum of ionic current, a sustained spray, and an efficient ionization at 3 kV ESI and 100 V sampling cone voltages. After 4 min of signal acquisition at a flow rate of 200 nL/min a spectrum of high S/N was obtained (Fig. 5), although a fair S/N was observed already after 60 scans (30 s). A reproducible compositional mapping of eight GT1 molecular components, reflecting different lipid variants in the fraction, was obtained from both triply and doubly charged molecular ions. Interestingly, three minor GT1 molecular species not detectable by capillary infusion could be documented by the low-abundant molecular ions at *m/z* 1094.20, 1108.20, and 1109.21, assigned by calculation to GT1 (d18:1/21:1), GT1 (d18:1/23:1), and GT1 (d18:1/23:0), respectively.

In the same study [27], the thin chipESI/QTOF-MS was explored to address the fundamental issue of efficient fragmentation analysis by CID-MS/MS of ganglioside species, known to require an extended signal acquisition time under variable collision energies to generate enough

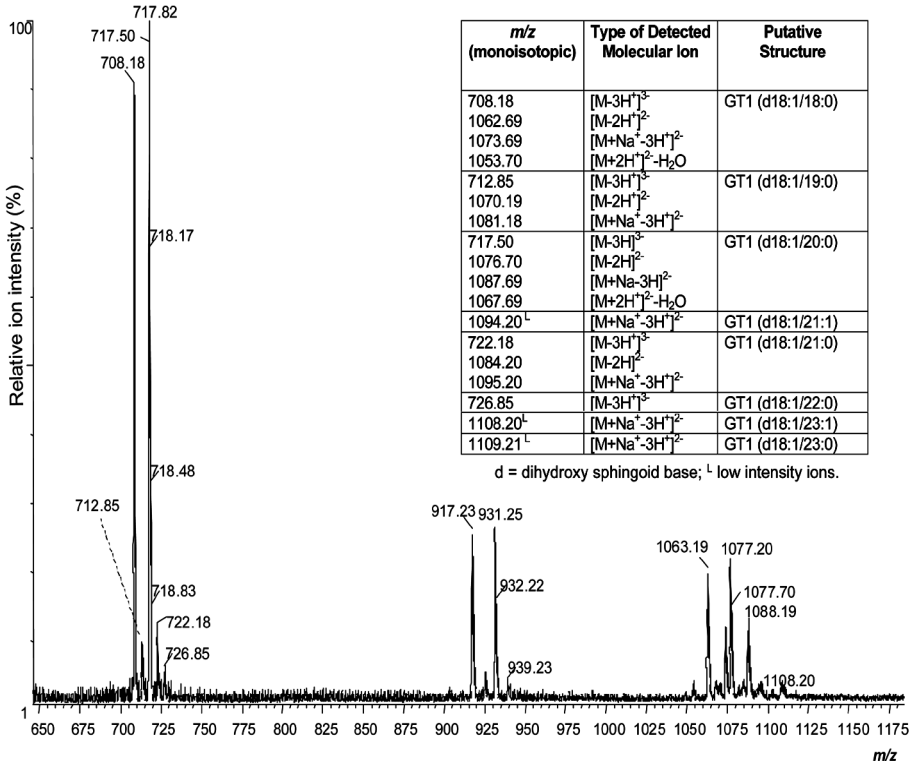

m/z (monoisotopic)	Type of Detected Molecular Ion	Putative Structure
708.18	$[M-3H^+]^{3-}$	GT1 (d18:1/18:0)
1062.69	$[M-2H^+]^{2-}$	
1073.69	$[M+Na^+-3H^+]^{2-}$	
1053.70	$[M+2H^+]^{2-}-H_2O$	
712.85	$[M-3H^+]^{3-}$	GT1 (d18:1/19:0)
1070.19	$[M-2H^+]^{2-}$	
1081.18	$[M+Na^+-3H^+]^{2-}$	
717.50	$[M-3H]^{3-}$	GT1 (d18:1/20:0)
1076.70	$[M-2H]^{2-}$	
1087.69	$[M+Na-3H]^{2-}$	
1067.69	$[M+2H^+]^{2-}-H_2O$	
1094.20[L]	$[M+Na^+-3H^+]^{2-}$	GT1 (d18:1/21:1)
722.18	$[M-3H^+]^{3-}$	GT1 (d18:1/21:0)
1084.20	$[M-2H]^{2-}$	
1095.20	$[M+Na^+-3H^+]^{2-}$	
726.85	$[M-3H^+]^{3-}$	GT1 (d18:1/22:0)
1108.20[L]	$[M+Na^+-3H^+]^{2-}$	GT1 (d18:1/23:1)
1109.21[L]	$[M+Na^+-3H^+]^{2-}$	GT1 (d18:1/23:0)

d = dihydroxy sphingoid base; [L] low intensity ions.

Figure 5. Microchip ESI/QTOF MS1 of a ganglioside fraction derived by combining the TIC MS scans at 3 kV ESI voltage and 100 V sampling cone potential. (a) *m/z* range: (650–1175). Inset: the compositional mapping of the purified native GT1 ganglioside fraction (exhibiting HPTLC migration properties of the GT1b species) separated from the total ganglioside mixture isolated from adult human brain tissue as detected by (−)microchip ESI-QTOF-MS1. Reproduced and adapted by permission of The Royal Society of Chemistry [27].

fragment ions for high sequence coverage. By this novel approach, the instability of the electrospray and/or signal interruption, frequently reported in the case of capillary-based ESI [44], could be overcome, and a stable TIC MS/MS was shown to be crucial for different sequencing events. A triply charged ion at *m/z* 717.50, corresponding to the GT1 (d18:1/20:0), could be successfully sequenced (Fig. 6). The fragmentation process gave rise to sialylated fragment ions indicative for the carbohydrate sequence of the GT1, as well as for characterization of its ceramide portion. The complete fragmentation pattern of the molecule (Fig. 7) could be deduced from the abundant Y- and Z-type ions formed from the nonreducing end, while the X-type ring cleavages appeared at lower abundance. Informative C- and B-type ions observed to be similarly favored under given conditions were obtained. Moreover, a number of fragment ions deriving from different sugar portion GT1 isomers, in particular *m/z* 364.09 ($B_{2\alpha}$), 966.39 $^{2,4}X_{2\alpha}$ specific for GT1c, and *m/z* 493.10 ($B_{2\alpha}/B_{1\alpha}$) specific for GT_{α}, respectively, could be clearly discriminated here, supporting the presence of structural isomers or isobars as distinct species.

3 Fully automated chip-based electrospray MS

3.1 Coupling of the fully automated chip-based nanoESI system to high-performance MS for carbohydrate analysis

NanoMate™ 100 (Advion BioSciences), the world's first fully automated nanoelectrospray system, is a robotic device that provides an automated nanoelectrospray ion source for mass spectrometers [8]. In this system, by an automatic infusion, samples at low flow rates (50–100 nL/min) are admitted directly into MS [9, 10]. In addition to the robot itself, the key component of the system is the ESI chip. The robot holds a 96-well sample plate and a 96-pipette tip tray. Automated sample analysis is achieved by loading a disposable, conductive pipette tip on a movable sampling probe, aspirating sample *via* a syringe pump, and moving the sampling probe to engage against the back of the ESI chip. ESI process is initiated by applying a head pressure and voltage to the sample in the pipette tip. Each nozzle and tip is used only once in

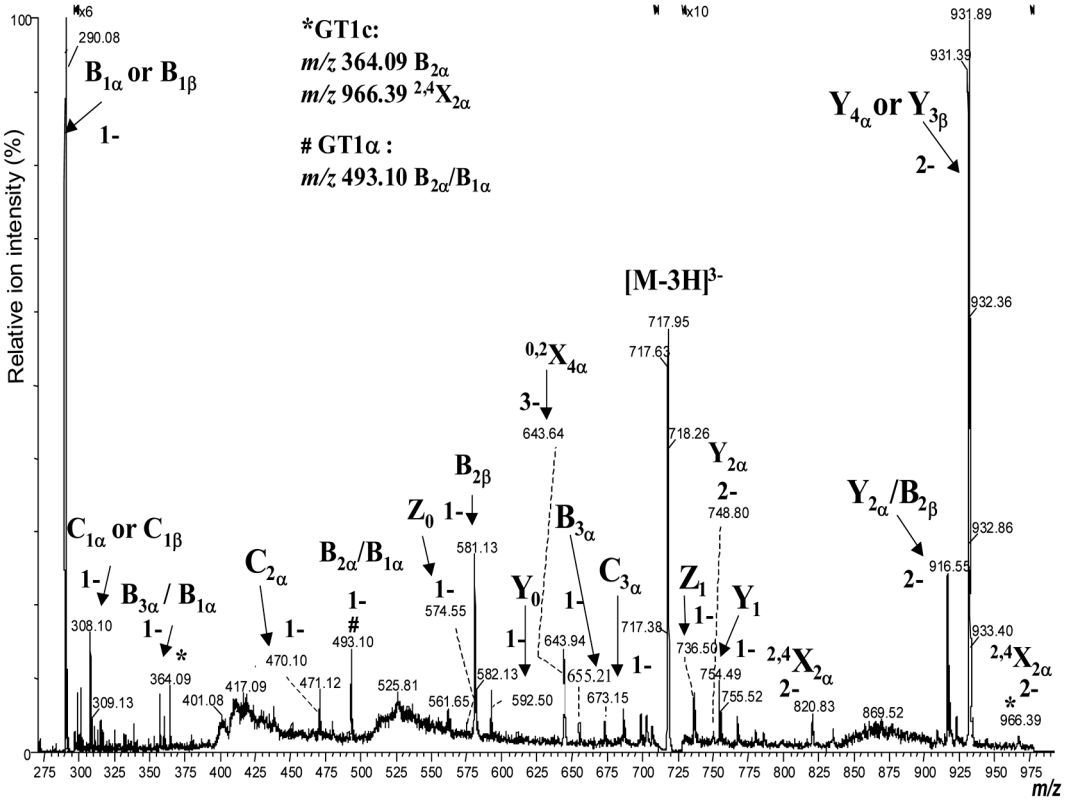

Figure 6. Microchip ESI/QTOF-MS/MS of the triply charged ion at *m/z* 717.50 corresponding to GT1 (d18:1/20:0). ESI voltage: 3 kV. Sampling cone potential: 100 V. Spectrum is derived by combining the scans corresponding to 40 and 70 eV in the TIC MS/MS. Nomenclature for assignment of fragment ions is according to [63–65]. Reproduced by permission of The Royal Society of Chemistry [27].

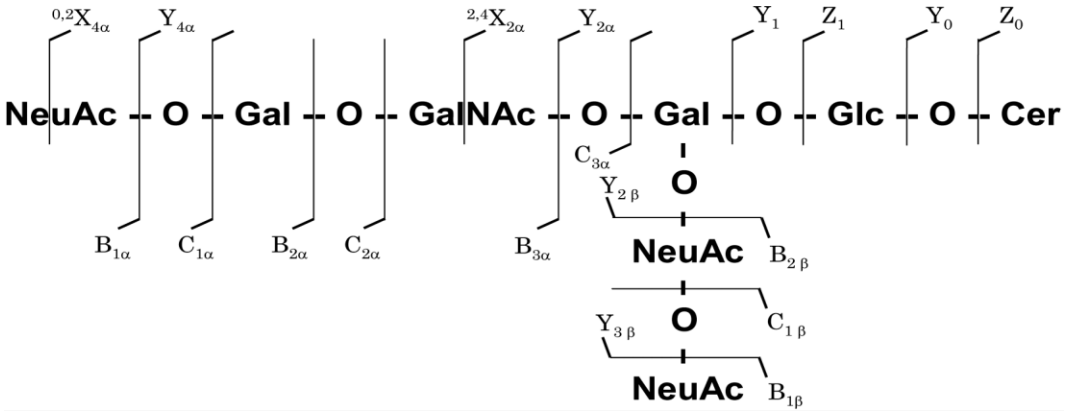

Figure 7. Structure and the corresponding fragmentation scheme of the GT1b species. Product ions detected from the spectrum depicted in Fig. 6 are assigned. Nomenclature for assignment of fragment ions is according to [61–65]. Reproduced by permission of The Royal Society of Chemistry [27].

order to eliminate carryover and contamination typical to conventional autosamplers. The ESI chip is an array of nanoESI nozzles of 10 μm internal diameter etched in a planar silicon chip. The chip is fabricated from a monolithic silicon substrate using deep reactive ion etching (DRIE) and other standard microfabrication techniques [7]. The inert coating on the surface allows a variety of acidic and organic compositions and concentrations to be used to promote ionization without any degradation of the nozzle [7]. As visible in Fig. 8, a channel extends from the nozzle through the microchip.

In conventional electrospray devices the electric field is defined by the potential difference between the ESI tip (fluid potential) and the mass spectrometer inlet. A unique feature of the ESI chip is the incorporation of the ESI ground potential into the spray nozzle so that the electric field around the nozzle tip is formed from the potential difference between the conductive silicon substrate and the voltage applied to the fluid *via* the conductive pipette tip [7–11]. In such a configuration, the distance that defines the electric field is about 1000 times shorter than the one between the nozzle and mass spectrometer. Therefore, the mass spectrometer position and voltage, though crucial for efficient ion transfer into analyzer, do not play any role in formation of the chip electrospray, thus essentially decoupling the ESI process from the inlet of the mass spectrometer.

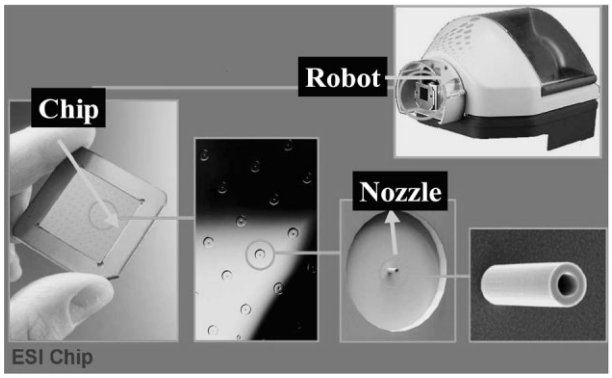

Figure 8. NanoMate™ 100 incorporating ESI chip technology. Courtesy of Advion BioSciences.

For carbohydrate analysis, the NanoMate robot was first mounted onto the QTOF and IT mass spectrometers [47–49] *via* special brackets, allowing adjustment of the robot position with respect to the sampling cone. Recently, the first coupling of the NanoMate robot to the FTICR-MS at 9.4 T and sustained off-resonance CID (SORI CID) MS/MS was reported [50]. The new assembly was optimized in the negative ion mode to combine automated sample delivery on the chip along with maximal sensitivity, ultra-high-resolution, accurate mass determination provided by the FTICR instrument, and efficient MS/MS in one system. In this study a specially designed interface was constructed by Bruker Daltonik (Bremen, Germany) in order to obtain a viable coupling of the NanoMate system to the Bruker Apex II Apollo ion source. An interesting coupling feature derived from the NanoMate ionization principle was the possibility to initiate and maintain a constant electrospray under a very low, if any, voltage on the metal-coated glass capillary of the FTICR instrument.

3.2 Applications

3.2.1 Complex biological mixtures of glycopeptides

The feasibility and analytical potential of the fully automated chip-based ESI/QTOF-MS for high-performance glycoscreening, sequencing, and identification was for

the first time explored on a complex glycopeptide mixture of *O*-glycosylated sialylated amino acids and peptides obtained from urine of a patient suffering from Schindler disease [48]. Using the negative ion mode detection and methanol as a solvent, the NanoMate provided a sample infusion at 100 nL/min flow rate. For a sample concentration of approximately 2–3 pmol/μL, spectra of high S/N were obtained within less than 1 min of acquisition, indicating a two to three times higher sensitivity than the one obtained in a similar study by using the conventional capillary-based nanoESI in Z-spray geometry (unpublished results).

The reduced S/N of low-abundant molecular precursor ions in complex mixtures obtained by classical nanoESI-MS/MS can generally be overcome by extended accumulation in an off-line approach [44], but it is frequently hindered by spray and/or signal instability. The performance of the NanoMate system to provide long-lasting electrospray signal, rendered reliable conditions for high sensitivity, particularly useful for detection and sequencing of minor glycopeptide components, previously accessible for fragmentation from such complex mixtures only by the on-line CE/ESI-QTOF-MS [33].

Singly and doubly charged ions derived from tri- to octasaccharide peptides or free oligosaccharides were detected, originating from tri- (singly charged), tetra- (singly and doubly charged), penta- (doubly charged), and hexasaccharide (doubly charged) *O*-linked either to Ser or Thr, whereas species from hepta- and octasaccharide peptides were observed as less abundant doubly charged pseudomolecular ions. A large number of minor sialylated oligosaccharide components were identified as well. A low-abundant doubly charged ion detected at *m/z* 890.32 in MS1 was subjected to the chip nanoESI-MS/MS by CID at low collision energies (Fig. 9) and, accordingly, the fragmentation pattern (Fig. 10) could be identified and assigned to the octasaccharide $Neu5Ac_2Gal_{32}GalNAc$-Ser. All these data demonstrated for the first time the ability of the NanoMate chipESI/QTOF-MS methodology to identify minor glycoconjugate species, or those having labile attachments like sialic acid previously undetectable by ESI–MS only [33].

The off-line CE-MS method is considered in some cases a convenient approach due to its higher flexibility toward system optimization than the one provided by the on-line

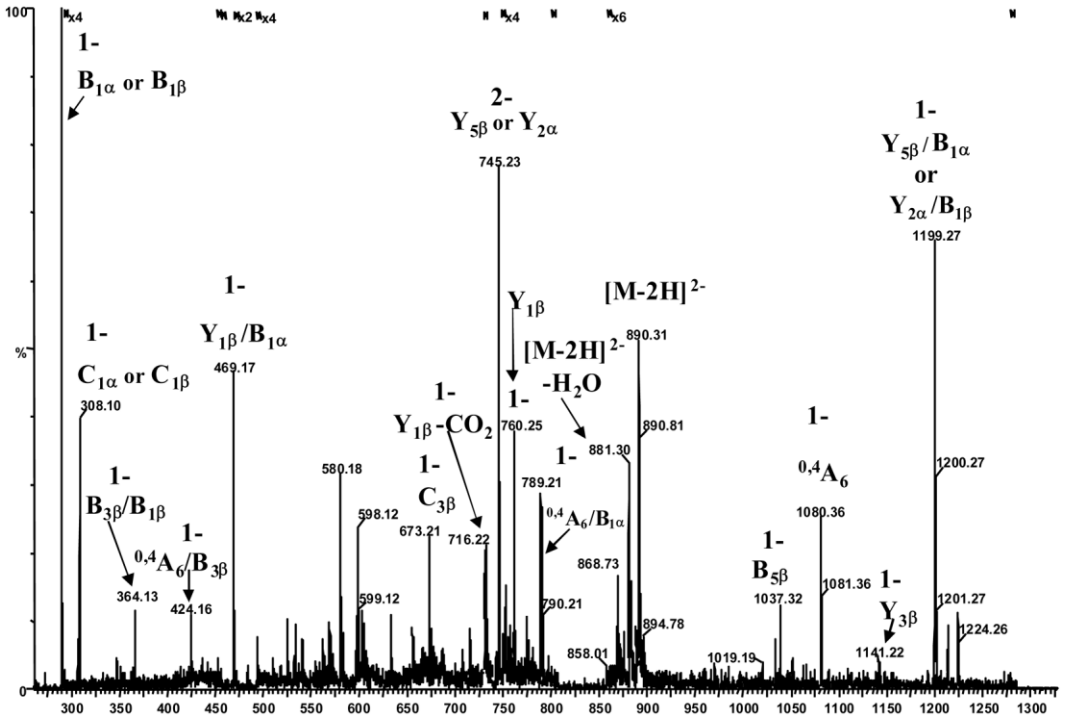

Figure 9. Automated chip-based (−)nanoESI/QTOF-MS/MS of $Neu5Ac_2Gal_3GlcNAc_2GalNAc$-Ser detected as a doubly charged ion at *m/z* 890.32. Spectrum is the sum of scans at collision energy 40 and 70 eV. Number of scans: 200. Average sample concentration: 3 pmol/μL. Average sample consumption for the MS/MS experiment: 2 pmol. Nomenclature for assignment of fragment ions is according to [61, 62]. Reprinted from [47], with permission.

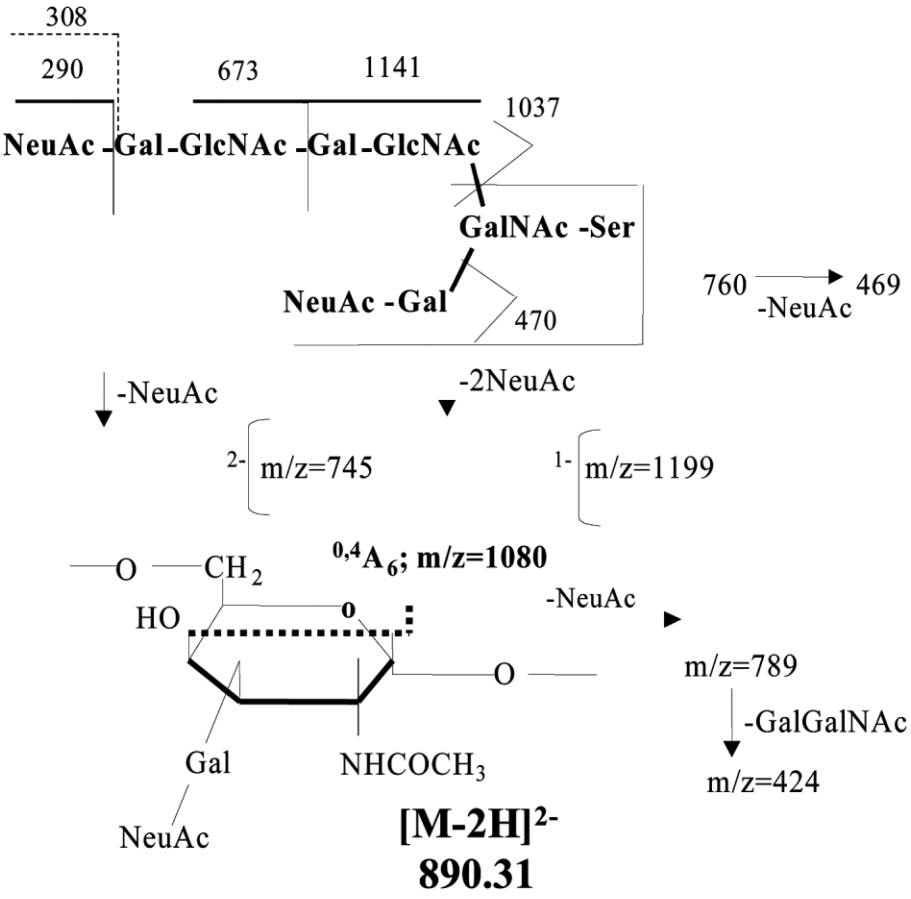

Figure 10. Fragmentation scheme of $Neu5Ac_2Gal_3GlcNAc_2GalNAc$-Ser detected as a doubly charged ion at *m/z* 890.31. Reprinted with permission from [47].

methods. For this reason, the off-line coupling of CE to (−)nanoESI-QTOF-MS has been lately intensively developed and implemented for glycoconjugate analysis. Its potential for separation, screening, and structural elucidation of different types of glycoconjugates, such as glycosaminoglycans [51, 52], *O*-glycosylated peptides [53], and gangliosides [54], was demonstrated in detail. However, using the CE instrument as a fraction collector, the sample concentration is lowered because sample reservoirs contain electrolyte, so that volumes of a few nanoliters are diluted into tens-of-microliters. Lack of sensitivity is therefore a major drawback of this approach.

The second limitation of the off-line approach is the low throughput, as a consequence of both the time-consuming collection of fraction and the additional treatments of the sample sometimes necessary to be applied prior to MS. Among the postseparation treatments, increasing the sample concentration by solvent evaporation is the most frequent and time-consuming one. These two inherent problems associated to the off-line CE-MS coupling could be to a significant extent overcome by automated chip-based negative ion ESI-QTOF-MS in off-line conjunction with CE [55]. In this study, for testing the compatibility of the off-line CE coupling to the (−)nano ESIchip NanoMate/QTOF-MS for ionization and detection in a given CE buffer system, a multicomponent mixture of *O*-glycosylated amino acids and peptides from urine of patients suffering from Schindler disease was dissolved in 0.1 M formic acid/ammonia pH 2.8 to a concentration of 5 pmol/μL and infused automatically into MS. A constant and stable spray over 10 min analysis time and high ionic current indicated the compatibility of this buffer system with automatic chip-based ESI and that the analyte molecules could be efficiently ionized. In addition, the flow rate under these buffer conditions was found reduced to 75 nL/min. Following the CE-UV analysis in the reverse polarity, CE fractions were collected, loaded onto the 96-well plate of the robot, and automatically subjected to the (−)nanoESIchip NanoMate/QTOF-MS and MS/MS (Fig. 11) without the need of preconcentration or any other postseparation treatment which would significantly increase the experiment time. Two major doubly charged ions at *m/z* 525.28 and 532.29 accompanied by their respective singly charged counterparts at *m/z* 1051.23 and 1065.23 corresponding to Ser- and Thr-linked $Neu5Ac_2HexHexNAc$ (HexNAc = *N*-acetyl hexosamine) have been separated and detected in the

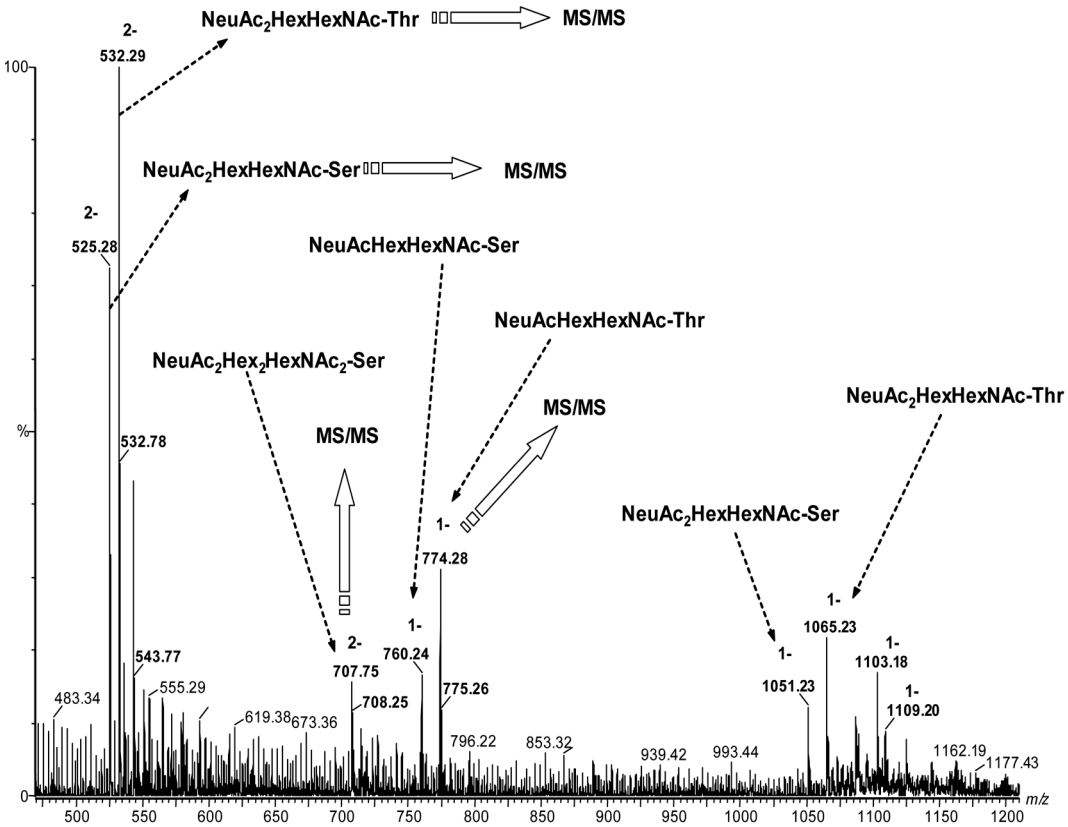

Figure 11. (−)NanoESIchip/QTOF mass spectrum of the second CE-collected fraction at 80 min after injection. Solvent: 0.1 M formic acid buffered with ammonia to pH 2.8; fraction/buffer concentration: ~3 pmol/μL. Number of scans: 100. Average sample consumption for MS experiment: 0.4 pmol. Copyright © 2004 John Wiley & Sons. Reproduced with permission from [55].

second CE fraction. Ser- and Thr-linked Neu5AcHexHexNAc were also observed as singly charged ions at *m/z* 760.24 and 774.28, respectively. In lower abundance, the Ser-linked $Neu5Ac_2Hex_2HexNAc_2$ was detected as a doubly charged ion at *m/z* 707.75. Although previously [53] the off-line CE/MS was reported to require rather high amounts of glycopeptide sample for detection, the final concentration of the fraction was here approximately 3 pmol/μL. In the case of ammonium formate, the 75 nL/min flow rate exhibited by the NanoMate chip system yielded a fair S/N by only 30 scans of signal accumulation (Fig. 11) under the sample consumption of approximately 0.4 pmol, which is a superior sensitivity in comparison with the capillary-based experiments [53, 54]. Due to the high spray stability, the MS/MS investigation of a low abundant doubly charged ion at *m/z* 707.75 attributed to $Neu5Ac_2Hex_2HexNAc_2$-Ser was greatly enhanced (Fig. 12). The low signal intensity corresponding to this ion could be compensated by the longer acquisition time (15 min) of the MS/MS signal. By this procedure, a sufficient number of sequence ions for clear-cut structural elucidation of the molecule could be generated and detected (Fig. 13). It is noteworthy to mention that in this study, the total amount of sample consumed for generating one MS and three MS/MS of high S/N and sufficiently informative was only 12 pmol.

In another study, the newly conceived NanoMate/FTICR coupling was tested for screening and sequencing by sustained off-resonance (SORI)-CID of *O*-glycosylated peptides and amino acids extracted from urine of a patient suffering from Schindler disease and from urine of a healthy age-matched individual for comparative analyses [50]. The mixtures were dissolved in methanol to different concentrations and transferred onto the glass microtiter plate of the NanoMate robot. The highest sensitivity obtained in this set of experiments was 0.5 pmol/μL, which represents a value with one order of magnitude higher than the one achieved in a similar study carried out by using capillary ESI infusion in the same Apollo Apex II configuration [32]. For the initiation of the chip spray, the fine tuning on the *x*-, *y*-, and *z*-axes of the chip nozzle toward the FTICR-MS inlet has been reported to be a critical step [50]. In addition, it was shown that a significant

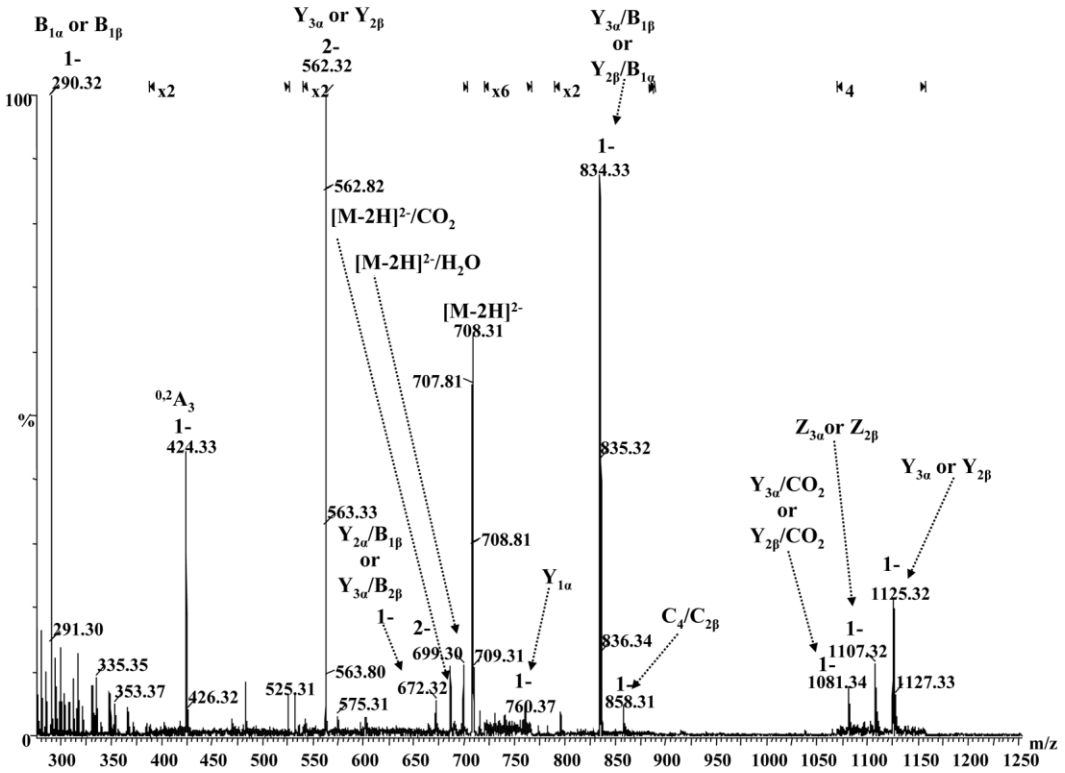

Figure 12. (−)NanoESIchip/QTOF-MS/MS of the doubly charged ion at *m/z* 707.75 assigned to $Neu5Ac_2Hex_2HexNAc_2$-Ser detected in the second CE-collected fraction. Collision energy: 20–40 eV; collision gas pressure: 12 psi. For precursor ion isolation, LM (low-mass resolution) and HM (high-mas resolution) parameters were set at 10 and 10, respectively. Number of scans: 400. Average sample consumption for MS/MS experiment: 3 pmol. Nomenclature for assignment of fragment ions is according to [61, 62]. Reproduced from [55], with permission.

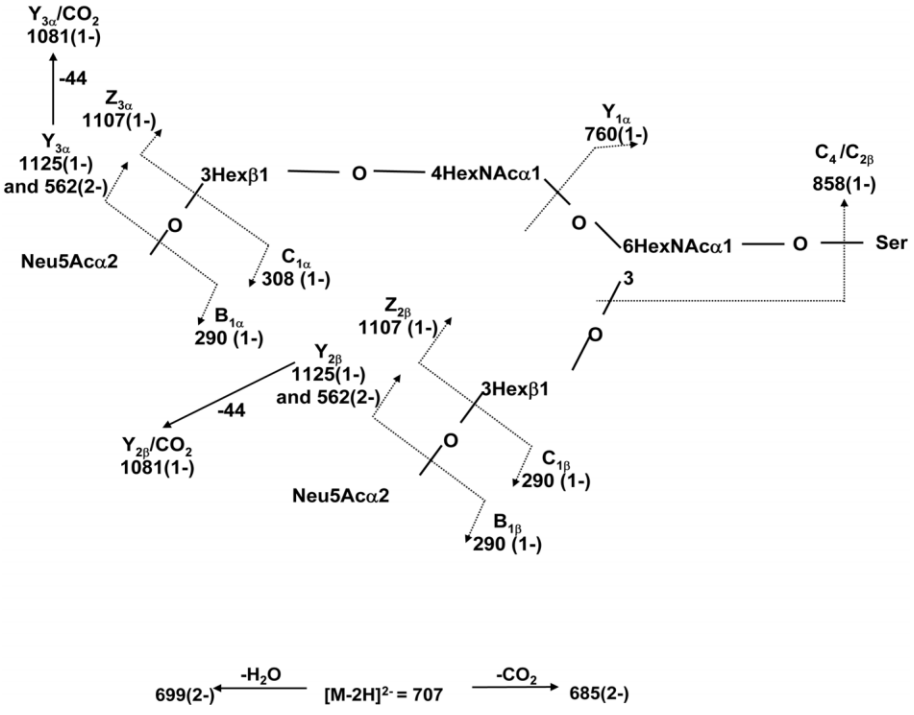

Figure 13. Fragmentation scheme of the doubly charged ion at *m/z* 707.75 assigned to $Neu5Ac_2Hex_2HexNAc_2$-Ser detected in the second CE-collected fraction. Nomenclature for assignment of fragment ions is according to [61, 62]. Reproduced from [55], with permission.

increase of the spray stability and intensity of the MS signal could be achieved by applying a low potential of 50 V to the ion transfer capillary of the FTICR-MS instrument.

In Fig. 14, the (−)chipESI/FTICR-MS of an *O*-glycopeptide mixture from patient's urine is depicted, where a significantly higher number (50) of components than previously detected [32] was found. These glycoforms were in general Ser- and Thr-linked disialo saccharides expressing various saccharide chain lengths ranging from tetra- to octasaccharide. MS experiments carried out under the same conditions of sample solution and ionization/detection indicated a run-to-run and nozzle-to-nozzle reproducibility of nearly 100%. The particular advantage of the NanoMate system to exhibit a high ionization yield and a preferential formation of multiply charged ions is clearly illustrated by the spectrum in Fig. 14. In comparison with previously reported data obtained by regular capillary-based (−)nanoESI-FTICR-MS on a similar glycopeptide mixture [32], the (−)nanoESIchip/FTICR-MS was found to provide a higher ionization efficiency of even less abundant glycopeptide species. In addition, by (−)nanoESIchip/FTICR-MS a considerable number of triply charged ions could be formed and detected under a high S/N, whereas by capillary-based (−)nanoESI-FTICR-MS no triply charged glycopeptide ions were formed/detected [32].

Moreover, four new components, not identified by any other method before [32–35], were detected by this novel approach and identified under a high mass accuracy: to sodiated Ser- and Thr-linked (disialo) octasaccharides and (trisialo) undecasaccharides, respectively (Fig. 14).

For identification of potential diagnostic marker components, a mixture of *O*-glycopeptides extracted from urine of an age-matched healthy control person, identically prepared as described before, was subjected to (−)ESI-chipNanoMate/FTICR-MS and SORI-CID MS/MS under the same experimental conditions as those from patient urine [50]. The MS pattern was different: in this mixture a reduced number of glycoconjugate species has been found, where those with shorter chains and lower degree of sialylation were dominating. By the NanoMate/FTICR SORI-CID MS/MS experiment, the structure of the Ser-linked (disialo) hexasaccharide components could be straightforwardly determined.

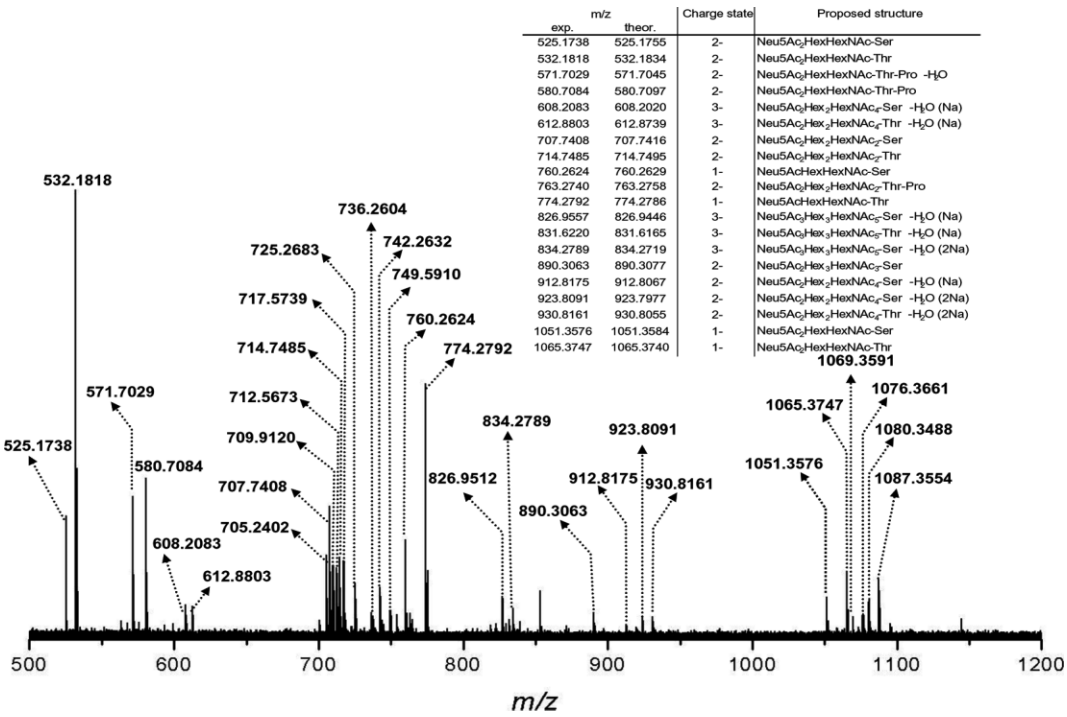

m/z exp.	m/z theor.	Charge state	Proposed structure
525.1738	525.1755	2-	$Neu5Ac_2HexHexNAc$-Ser
532.1818	532.1834	2-	$Neu5Ac_2HexHexNAc$-Thr
571.7029	571.7045	2-	$Neu5Ac_2HexHexNAc$-Thr-Pro -H_2O
580.7084	580.7097	2-	$Neu5Ac_2HexHexNAc$-Thr-Pro
608.2083	608.2020	3-	$Neu5Ac_2Hex_2HexNAc_4$-Ser -H_2O (Na)
612.8803	612.8739	3-	$Neu5Ac_2Hex_2HexNAc_4$-Thr -H_2O (Na)
707.7408	707.7416	2-	$Neu5Ac_2Hex_2HexNAc_2$-Ser
714.7485	714.7495	2-	$Neu5Ac_2Hex_2HexNAc_2$-Thr
760.2624	760.2629	1-	Neu5AcHexHexNAc-Ser
763.2740	763.2758	2-	$Neu5Ac_2Hex_2HexNAc_2$-Thr-Pro
774.2792	774.2786	1-	Neu5AcHexHexNAc-Thr
826.9557	826.9446	3-	$Neu5Ac_2Hex_3HexNAc_5$-Ser -H_2O (Na)
831.6220	831.6165	3-	$Neu5Ac_2Hex_3HexNAc_5$-Thr -H_2O (Na)
834.2789	834.2719	3-	$Neu5Ac_2Hex_3HexNAc_5$-Ser -H_2O (2Na)
890.3063	890.3077	2-	$Neu5Ac_2Hex_3HexNAc_2$-Ser
912.8175	912.8067	2-	$Neu5Ac_2Hex_2HexNAc_4$-Ser -H_2O (Na)
923.8091	923.7977	2-	$Neu5Ac_2Hex_2HexNAc_4$-Ser -H_2O (2Na)
930.8161	930.8055	2-	$Neu5Ac_2Hex_2HexNAc_4$-Thr -H_2O (2Na)
1051.3576	1051.3584	1-	$Neu5Ac_2HexHexNAc$-Ser
1065.3747	1065.3740	1-	$Neu5Ac_2HexHexNAc$-Thr

Figure 14. Automated (−)chipESI/FTICR mass spectrum of a fraction from urine of patients suffering from Schindler disease. Apex II metal-coated glass capillary voltage: 50 V. Capillary exit: −79 V. Sample concentration: 5 pmol/μL in methanol. Number of scans: 150. Average sample consumption for MS experiment: 2.5 pmol. Inset: Table: Ions detected and identified with a mass accuracy below 12 ppm in the mixture of *O*-glycosylated peptides at 5 pmol/μL. Nomenclature for assignment of fragment ions is according to [61, 62]. Reproduced and adapted with permission from [50].

3.2.2 Combination of fully automated chip ESI-MS and automated software assignment for identification of heterogeneous mixtures of *N*-, *O*-glycopeptides, and oligosaccharides

A urine fraction containing sialylated carbohydrates from a patient presenting a clinical picture associated congenital disorders of glycosylation (CDG) was submitted to glycoscreening by fully automated chip-based (−)nanoESI/QTOF-MS [47]. The sample with average concentration of 5 pmol/μL in methanol was loaded onto the 96-well plate of the NanoMate robot. Following automatic infusion, the mass spectrum acquired for 3 min displayed a high level of heterogeneity concerning the type of glycans and glycopeptides, as well as the degree of sialylation (Fig. 15). For preliminary analysis and assignment of glycoforms, a computer algorithm for calculation of glycoconjugate composition was developed [47, 56] thus providing the first two-stages platform for completely automatic and high-throughput analysis: (1) robotized sample delivery and infusion into MS followed by (2) automatic identification of components using software-assisted assignment. The experimental data for the input were the *m/z* values and the respective charge states provided by chip MS and MS/MS experiments. The capacity of the computer program was to calculate and propose all possible structures containing hexose (Hex), HexNAc, deoxyhexose (dHex), and Neu5Ac as monosaccharide building-block units. In the second step, the modeling of the theoretical fragmentation pattern from different structures with the same *m/z* was processed. The data were presented as a combination of ions B, C, Y, and Z, related to the cleavage of glycosidic bonds, as well as the A- and X-ring cleavage ions, aligned to the proposed structure of the chosen molecular ion. In Table 1 the software first-step MS analysis along with the proposed composition of single components from the chip-based (−)nanoESI/QTOF spectrum presented in Fig. 15 is given. The most prominent structures in the mixture were directly identified by this approach.

As an example, the doubly charged molecular ion at *m/z* 1008.74 (Fig. 15) showing the composition of either $Neu5Ac_2Hex_5HexNAc_3$ or $Neu5Ac_2Hex_3HexNAc_1dHex_5$ was submitted to the automated chip-based (−)nanoESI/QTOF-MS/MS by CID at low energies. The fragment ions of Neu5AcHex, Neu5AcHexHexNAc, $Neu5AcHex_2HexNAc$, and $Neu5Ac_2Hex_5HexNAc_2$ as C_2, C_3, C_4, and C_5 were assigned by this software to a truncated *N*-linked biantennary glycan missing the terminal HexNAc at the reducing terminus.

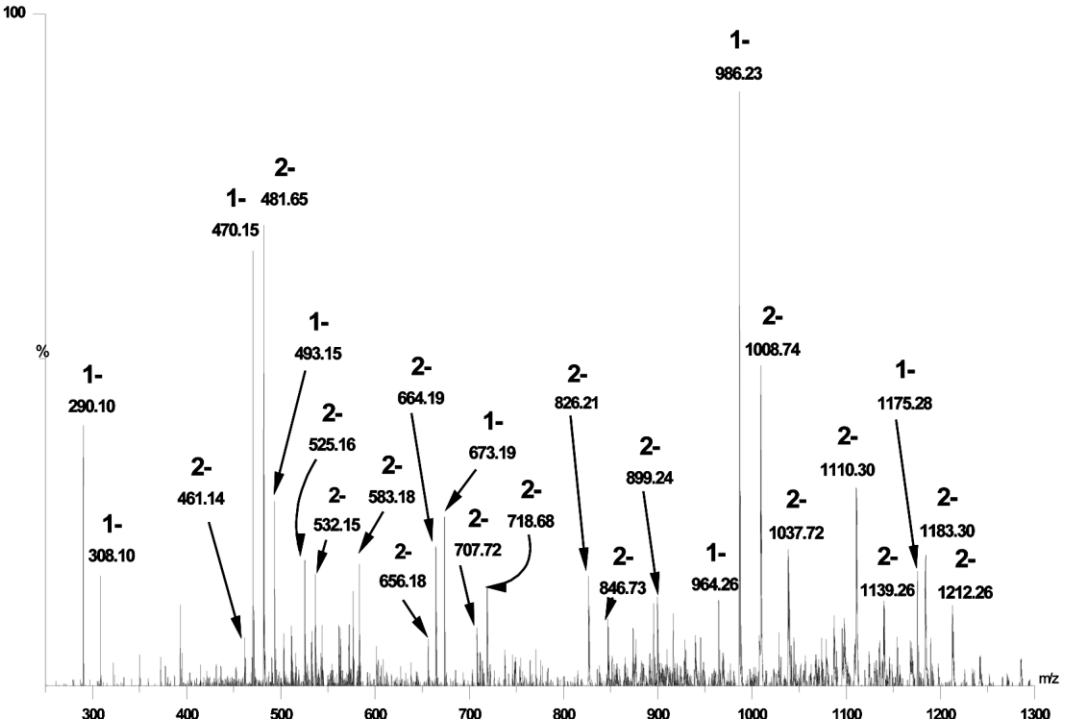

Figure 15. Fully automated chip-based (−)nanoESI/QTOF MS of the mixture containing glycans and glycopeptides from urine of a patient diagnosed with CDG. Average sample concentration: 5 pmol/μL; number of scans: 100. Average sample consumption for MS experiment: 2 pmol. Sampling cone potential: 50 V. Reprinted from [47], with permission.

Table 1. Computer-assisted assignment of the major ions detected by automated chip-based (−)nanoESI/QTOF-MS in the mixture of glycans and glycopeptides from urine of a patient diagnosed with CDG.

$[M - 2H]^{2-}$ *m/z*	$[M - H]^{-}$ *m/z*	Composition according to calculation	Theoretical *m/z*
	290.10	NeuAc (–H_2O)	290.09
	308.10	NeuAc	308.10
461.14		$NeuAc_2Hex_2$	461.15
	470.15	NeuAcHex	470.15
481.65		$NeuAc_2HexHexNAc$	481.66
	493.15	NeuAcHexNAc (–H_2O)	493.17
525.16		$NeuAc_2HexHexNAc$-Ser	525.18
532.15		$NeuAc_2HexHexNAc$-Thr	532.18
583.18		$NeuAc_2HexHexNAc_2$	583.20
656.18		$NeuAc_2dHexHexHexNAc_2$	656.23
664.19		$NeuAc_2Hex_2HexNAc_2$	664.23
	673.19	NeuAcHexHexNAc	673.23
707.72		$NeuAc_2Hex_2HexNAc_2$-Ser	707.74
718.68		$NeuAc_2Hex_2HexNAc_2$-Ser (Na)	718.74
826.21		$NeuAc_2Hex_4HexNAc_2$	826.28
846.73		$NeuAc_2Hex_3HexNAc_3$	846.80
899.24		$NeuAc_2dHexHex_4HexNAc_2$	899.31
	964.26	$NeuAc_2HexHexNAc$	964.33
	986.23	$NeuAc_2HexHexNAc$ (Na)	986.33
1008.74		$NeuAc_2Hex_5HexNAc_3$	1008.84
1037.72		$NeuAcdHexHex_5HexNAc_4$	1037.87
1110.30		$NeuAc_2Hex_5HexNAc_4$	1110.38
1139.26		$NeuAcdHexHex_5HexNAc_5$	1139.41
	1175.28	$NeuAc_2HexHexNAc$-Ser (2Na + P)	1175.32
1183.30		$NeuAc_2dHexHex_5HexNAc_4$	1183.41
1212.26		$NeuAcdHex_2Hex_5HexNAc_5$	1212.43

Reprinted from [47], with permission.

3.2.3 Characterization of *N*-glycosylation microheterogeneity and sites in intact glycoproteins

Glycosylation of proteins is one of the most ubiquitous post-translational modification. It is highly regulated and changes during differentiation, development, under different physiological and cell culture conditions, and in disease.

Diversity of glycoprotein structure resides on number and position of glycosylation sites within the polypeptide backbone and the type of sugar attached. Besides the microheterogeneity on the same glycosylation site, a number and type of glycan chain phosphorylation, sulfation, methylation, and acetylation may be found on glycan residues [57–59]. Therefore, a demand for a complete analysis of a single glycoprotein would have to provide information regarding microheterogeneity at single glycosylation sites as well as a structural characterization of the appropriate carbohydrate moiety.

Due to recent advances in automated chipESI-MS and the development of small-scale sample preparation procedures, the characterization of glycosylations became amenable to high-throughput experiments, in which the necessary sample amount was decreased to the low picomolar level. In the first study carried out for the determination of the glycosylation site by fully automated chip nanoESI-MS, the NanoMate 100 robot was coupled to the front of a Finnigan LTQ IT *via* a specially designed mounting bracket [49]. The tryptic digest of bovine pancreatic ribonuclease B was dissolved in 50% methanol with 0.1% formic acid for positive ion mode and in 50% methanol with 0.1% ammonium hydroxide for negative ion mode to the concentration of 1 pmol/μL. Five microliters of sample was loaded onto the 96-well plate of the robot and infused into the LTQ IT MS at a flow rate of 100 nL/min. From the full-scan MS the complex peptide mass fingerprint of ribonuclease B was derived. Several peptides were sequenced by MS/MS using collision energies of 20–25% and a maximum scan time of 50 ms in combination with the automated search program Bio-

Works 3.1 (Finnigan LCQ). Nine out of 14 possible tryptic peptides were identified, resulting in a protein sequence coverage of 87%. The unidentified ions, showing a pattern typical for high-mannose type of glycosylation, were subjected to multiple stage MS, up to MS^5. As shown in Fig. 16a by fully automated chip-based infusion in combination with multiple stage CID MS, spectra of high quality and rich in information related to protein glycosylation could be obtained. Since the *N*-glycopeptides tend to fragment mostly at their oligosaccharide portion, it is often difficult to gather the data necessary for the characterization of their amino acid sequence. In the case described here the amino acid sequence was obtained in the MS^4 experiment as illustrated in Fig. 16b.

Fully automated chip-based nanoESI coupled to Q-FTICR at 9.4 T was recently employed for the first direct identification of multiple *O*-glycosylation sites in hinge region (HR) of immunoglobulin A1 (IgA1) isolated from myeloma as reported by Renfrow *et al.* [60]. The method was designed to provide heterogeneity assay of the tryptic glycopeptide expressing various *O*-glycoforms and particularly detection and localization of the Gal-deficient IgA1 extracted, separated, and purified from myeloma IgA1 HR and the structural elucidation of the glycopeptides by means of electron capture dissociation (ECD)-, infrared multiphoton dissociation (IRMPD)-, and activated ion ECD (AI-ECD)-MS/MS. The optimization of the methodology in terms of sequencing analysis has been carried out on a mixture of synthetically obtained peptides and glycopeptides of the IgA1 HR type. The samples were prepared at a concentration of 5 mM in 1:1 water/methanol, 2% acetic acid and microelectrosprayed from an in-house made fused silica capillary at a flow rate of 300 nL/min. By employing IRMPD-MS/MS the assay of the peptide sequence could be achieved, while by ECD-MS/MS the glycosylation sites of single glycopeptide and/or mixture of glycosylated peptides was unambiguously determined. For the tryptic-isolated myeloma IgA1 HR glycopeptides, the samples were desalted by C_{18} ZipTip into 30 μL of a 4:1 ACN/water solution containing 0.1% formic acid, and submitted to microelectrospray and automated chip-based ESI-FTICR-MS and MS/MS. The (+)ESI-FTICR-MS of isolated IgA1 HR peptide features a series of triply charged ions separated by one-third of the masses of GalNAc and Gal units. This reveals on one hand the high heterogeneity of the differentially glycosylated species, and on the other hand it can be deduced that the in-source fragmentation is reduced almost to zero, since no ion corresponding to nonglycosylated species could be detected and identified. Based on the amino acid sequence of the isolated IgA1 HR determined by IRMPD-MS/MS, building-block analysis of the monosaccharide units, and high mass accuracy and resolution of the detection, the number of GalNAc and Gal residues attached to the peptide back bone could be predicted. This assessment indicated that two of the predicted glycopeptides could bear a Gal-deficient glycan part.

When applying the same sequencing protocol as for synthetic peptides and glycopeptides for analysis of the isolated IgA1 glycopeptides by IRMPD- and ECD-MS/MS, only a limited number of fragment ions could be generated. Therefore, a combined sequencing technique based on tandem IRMPD and ECD events, called AI-ECD, was optimized to provide the full set of diagnostic ions for the localization of glycosylation sites. Thus, the quadrupole and stored waveform inverse Fourier transform (SWIFT) isolated precursor ions were subjected for 300 ms to photon irradiation at 6.4 or 8 W laser power, followed immediately by electron irradiation event for 10–20 ms at cathode heating power of 11 W, which corresponds to an electron emission current of 300 nA. The AI-ECD FTICR MS/MS of an isolated $[V^{216}–L^{246}]$ containing four GalNAc and four Gal moieties, acquired under the optimized sequencing conditions, gave rise to unambiguous determination of the glycosylation sites of the disaccharide units GalNAc-Gal to T^{225}, T^{228}, S^{230}, S^{232}, respectively (Fig. 17). Based on the accurate ESI-FTICR-MS1 mass determination, two of the glycopeptides were predicted as Gal-deficient glycopeptides. The AI-ECD FTICR-MS/MS of the $[V^{216}–L^{246}]$ containing four GalNAc and three Gal residues, predicted within a mass accuracy of 3.6 ppm, is presented in Fig. 18. The product ions generated by the peptide bone cleavage uniquely localize three GalNAc-Gal residues at T^{225}, T^{228}, and S^{230}, and a GalNAc at S^{232} (Fig. 18).

3.2.4 Complex ganglioside mixtures

A recent study [48] was designed to assess the potential of the fully automated (−)nanoESIchip/QTOF-MS and automatic MS/MS for screening and sequencing of gangliosides extracted from normal human cerebellar gray matter. The highly complex ganglioside sample dissolved in 100% methanol was automatically infused under the premise of optimization of the ESI chip ionization yield for all single ganglioside components first at higher concentrations (15 pmol/μL) and elevated values of the ESI chip and sampling cone potentials. Such an approach has been already demonstrated [42, 44] to enhance the ionization yield of larger ganglioside species from human brain tissues. Under these solution and instrumental parameters major ganglioside variants were detected, but minor components and/or longer chains, assumed to be present in the mixture could, however, not be found. The conditions were further modified by diluting

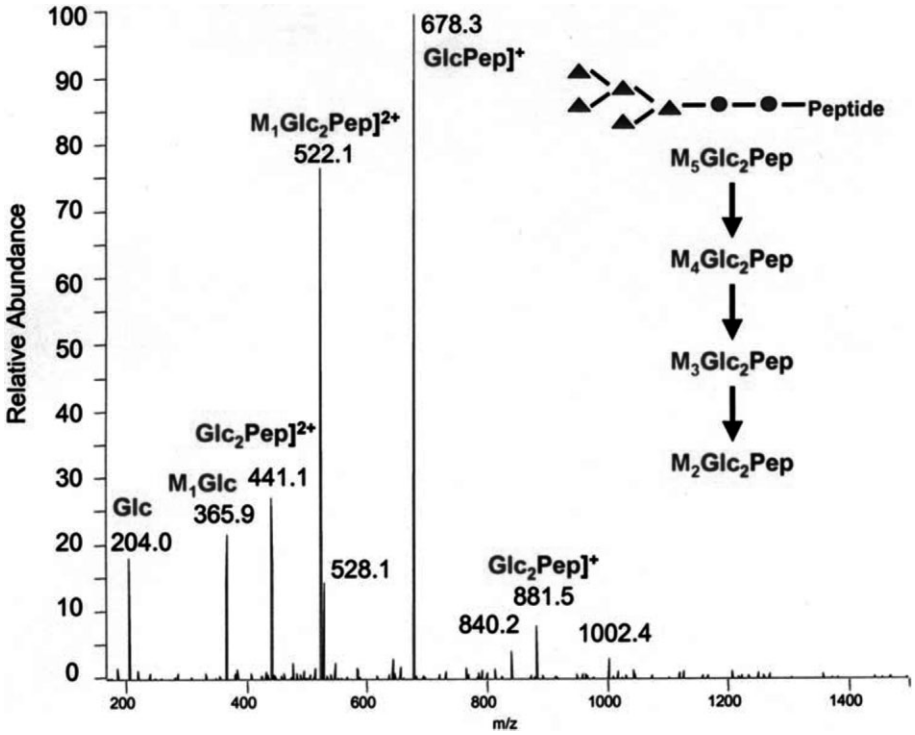

TABLE 1

Amino Acid Sequence and the Predicted Peptides from a Trypsin Digestion of Bovine Ribonuclease B

ETAAAK FER **QHMDSSTSAASSSNYCNQMMK** SR **NLTK** DR CK
PVNTFVHESLADVQAVCSQK **NVACK** **NGQTNCYQSYSTMSITDCR** **ETGSSK**
YPNCAYK **TTQANK** **HIIVACEGNPYVPVHFDASV**

Identified peptides are shown in bold; *N*-glycosylation site is shown in red.

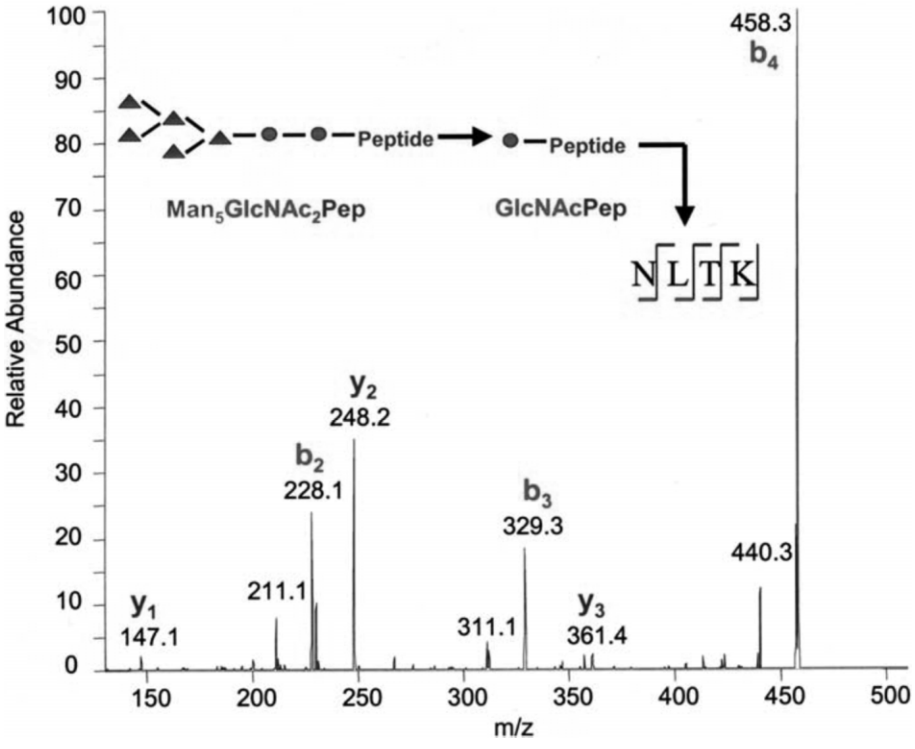

Figure 16. (a) Fully automated nanoESINanoMate/IT MS^5 for the stepwise removal of the mannose residue from the precursor ribonuclease B *N*-glycopeptide. (b) Fully automated nanoESINanoMate/IT MS^4 derived from ribonuclease B related *N*-glycopeptide for the identification of amino acid sequence. Inset: amino acid sequence and predicted peptides from tryptic digestion of ribonuclease B. Nomenclature for assignment of fragment ions is according to [66]. Reprinted and adapted with permission from [49].

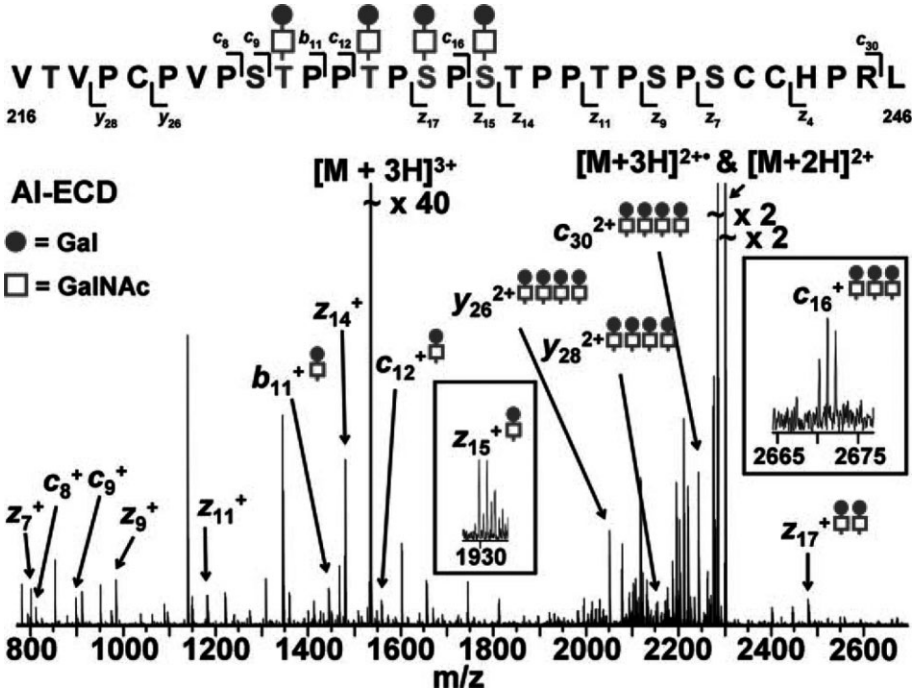

Figure 17. (+)ESI/AI-ECD FTICR-MS/MS spectrum of a population of [^{216}VTVPCOVPSTP-PTPSPSTPPTPSPSCCHPRL ^{246} + 4GalNAc + 4Gal + 3H]$^{3+}$ ions from the *O*-glycosylated IgA1 HR peptide. Isolation of the precursor ions: by quadrupole and SWIFT. IRMPD event: 300 ms photon irradiation at 6.4 or 8 W laser power. ECD event: 10–20 ms electron irradiation event at 11 W cathode heating power, ~300 nA. Nomenclature for assignment of fragment ions is according to [66]. Reprinted by permission of The American Society for Biochemistry and Molecular Biology from [60].

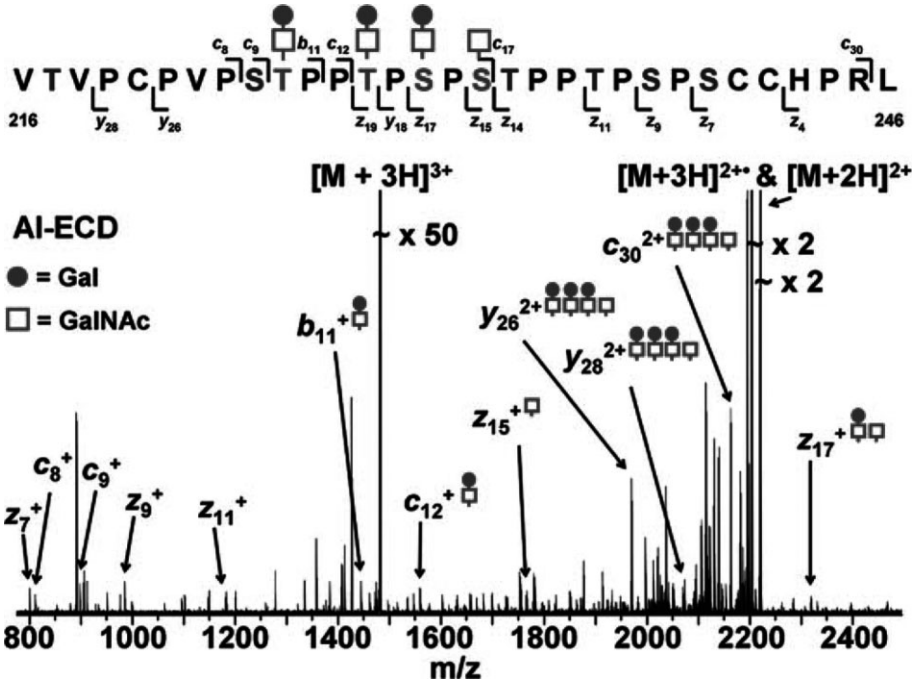

Figure 18. (+)ESI/AI-ECD FTICR-MS/MS spectrum of a population of [^{216}VTVPCOVPSTP-PTPSPSTPPTPSPSCCHPRL ^{246} + 4GalNAc + 3Gal + 3H]$^{3+}$ ions from the *O*-glycosylated IgA1 HR peptide. Isolation of the precursor ions: by quadrupole and SWIFT. IRMPD event: 300 ms photon irradiation at 6.4 or 8 W laser power. ECD event: 10–20 ms electron irradiation event at 11 W cathode heating power, ~300 nA. Reprinted by permission of The American Society for Biochemistry and Molecular Biology from [60].

the sample to 2–3 pmol/μL and varying the cone potential values from 45 to 135 V and the ESI capillary potential from 1.45 to 1.67 kV (Fig. 19), which allowed high ionization yield and detection of an extended number of species. By this approach, a realistic representation upon the ganglioside mixture heterogeneity as compared to data provided by TLC analysis was reported. According to this set of data, it was concluded that by ESIchip/MS a high sensitivity for the analysis of ganglioside multicomponent mixture, without compromising the ionization of minor, biologically relevant components can be achieved. Moreover, in this work the capability of the NanoMate chipESI to minimize in-source fragmentation and significantly reduce the analysis time as compared to ganglioside MS screening by capillary Z-spray sample infusion [42, 44] was demonstrated.

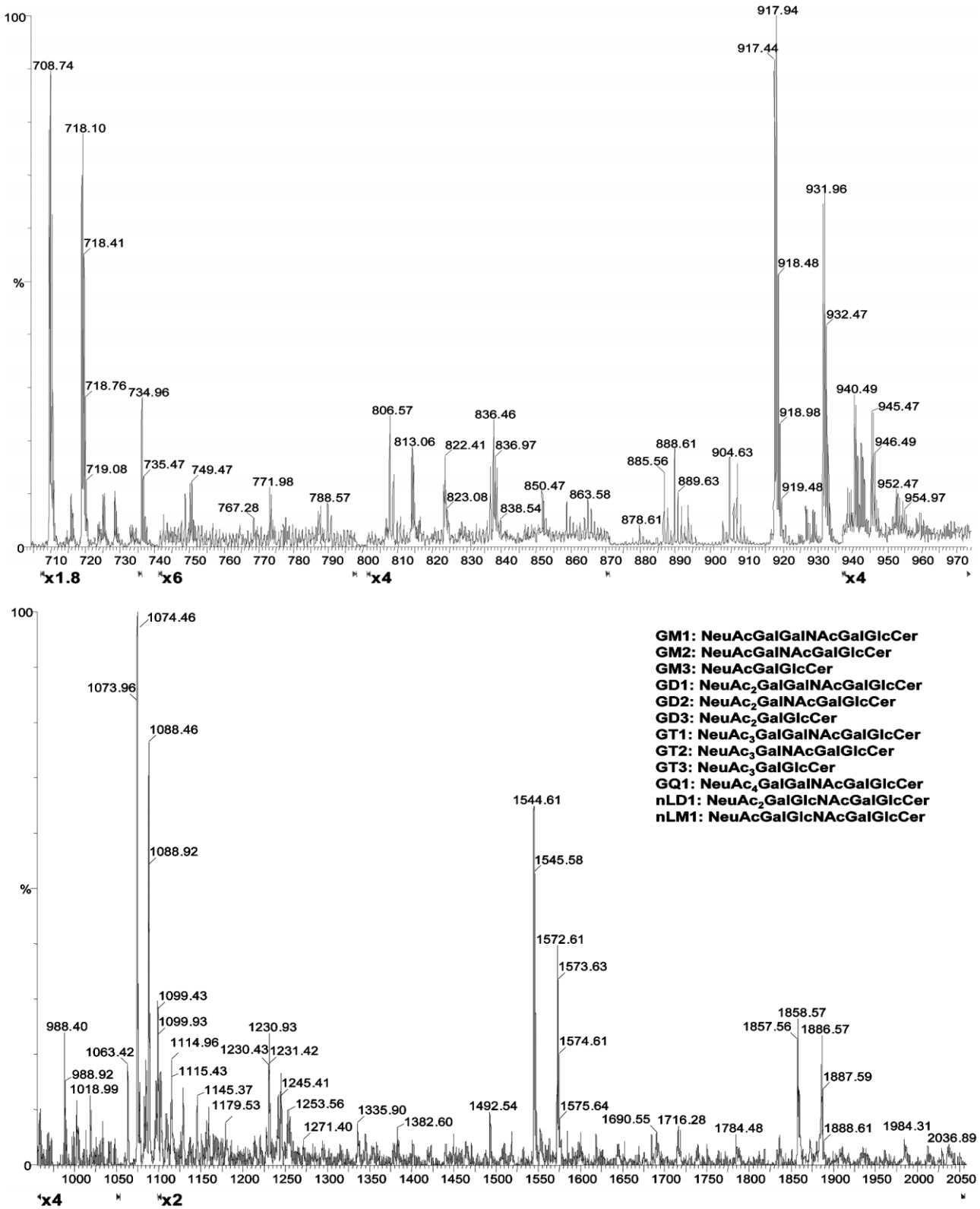

Figure 19. Fully automated (−)nanoESIchip/QTOF-MS of the native ganglioside mixture from normal human cerebellar gray matter. Sample concentration: 2–3 pmol/μL in methanol; acquisition time: 3 min; number of scans: 90. Average sample consumption for MS experiment: 0.7 pmol, sampling cone potential: 45–135 V. n.a. = not assigned. (a) *m/z* (700–980). (b) (980–2050). Reprinted and adapted by permission of Elsevier [48].

In Table 2, the assignment of singly, doubly, and triply charged ions corresponding to 44 different ganglioside components identified by automated chip-based nanoESI-QTOF-MS is listed. From Table 2, it is obvious that the cerebellar gray matter is dominated by GD1 glycoforms. GM1, GM2 and GM3, GD2 and GD3, as well as GT1 and GQ1 expressing different ceramide portions and biologically important *O*-acetylated and fucosylated GD1, and GT1 and GQ1 exhibiting high heterogeneity in their ceramide motifs could also be detected and identified by the NanoMate approach.

In order to test the feasibility of an efficient ganglioside sequencing by automated MS to MS/MS mode switching available on the QTOF mass spectrometer, the triply charged ion at *m/z* 708.39 assigned to GT1 (d18:1/18:0) has been submitted to automatic chip MS infusion followed by automatic MS/MS fragmentation in data-dependent acquisition (DDA). In previous work on ganglioside fragmentation using capillary-based (−)nanoESI-QTOF in Z-spray and manual selection for MS/MS [44], a long signal acquisition time with a sample consumption of about 50 pmol was necessary to obtain fairly high abundance of fragment ions diagnostic for the structure assignment of GT1 from a purified fraction. By Nano ESIchip-automatic fragmentation, within about 1 min of acquiring in MS/MS mode at a flow rate of 100 nL/min, approximately 0.5 pmol of material was sprayed and a sufficient set of fragment ions as fingerprints for structural elucidation of the molecule was obtained.

Table 2. Composition of single components in the ganglioside mixture from gray matter of normal human cerebellum as detected by a fully automated (−)nanoESIchip/QTOF-MS.

Type of molecular ion	*m/z* (monoisotopic)		Assigned structure
	Detected	Calculated	
$[M + 2Na - 4H]^{2-}$	611.40	611.35	GM3 (d18:1/18:0)
$[M - H]^{-}$	1179.57	1179.74	
$[M - H]^{-}$	1382.60	1382.82	GM2 (d18:1/18:0)
$[M - 2H]^{2-}$	734.96	734.91	GD3 (d18:1/18:0)
$[M + Na - 2H]^{-}$	1492.78	1492.81	
$[M - 2H]^{2-}$	748.99	748.93	GD3 (d18:1/20:0)
$[M - H]^{-}$	1518.51	1518.85	GM1, nLM1, and/or LM1 (d18:0/16:0)
$[M - 2H]^{2-}$	771.98	771.93	GM1, nLM1, and/or LM1 (d18:1/18:0)
$[M - H]^{-}$	1544.61	1544.85	
$[M - 2H]^{2-}$	786.00	785.92	GM1, nLM1, and/or LM1 (d18:1/20:0)
$[M - H]^{-}$	1572.61	1572.85	
$[M - H]^{-}$	1690.55	1690.93	Fuc-GM1(d18:1/18:0)
$[M - H]^{-}$	1716.56	1716.94	Fuc-GM1(d18:1/20:1)
$[M - 2H]^{2-}$	836.46	836.45	GD2 (d18:1/18:0)
$[M - 2H]^{2-}$	850.47	850.47	GD2 (d18:1/20:0)
$[M - 2H]^{2-}$	917.44	917.48	GD1, nLD1, and/or LD1 (d18:1/18:0)
$[M + Na - 3H]^{2-}$	928.45	928.47	
$[M - H]^{-}$	1835.62	1835.96	
$[M + Na - 2H]^{-}$	1857.56	1857.95	
$[M - 2H]^{2-}$	926.44	926.48	GD1, nLD1, and/or LD1 (t18:0/18:0)
$[M - 2H]^{2-}$	924.44	924.49	GD1, nLD1, and/or LD1 (d18:1/19:0)
$[M - 2H]^{2-}$	931.46	931.49	GD1, nLD1, and/or LD1 (d18:1/20:0)
$[M + Na - 3H]^{2-}$	942.44	942.48	
$[M - H]^{-}$	1885.60	1885.98	
$[M - 2H]^{2-}$	940.49	940.50	GD1, nLD1, and/or LD1 (t18:0/20:0)
$[M - 2H]^{2-}$	938.44	938.50	GD1, nLD1, and/or LD1 (d18:1/21:0)
$[M - 2H]^{2-}$	945.47	945.51	GD1, nLD1, and/or LD1 (d18:1/22:0)

Nomenclature for assignment of ions is according to [63–65]. Reprinted by permission of Elsevier from [48].

Table 2. Continued

Type of molecular ion	*m/z* (monoisotopic)		Assigned structure
	Detected	Calculated	
$[M - 2H]^{2-}$	954.46	954.51	GD1, nLD1, and/or LD1 (t18:0/22:0)
$[M - 2H]^{2-}$	952.47	952.52	GD1, nLD1, and/or LD1 (d18:1/23:0)
$[M - 2H]^{2-}$	958.46[a)]	958.52	GD1, nLD1, and/or LD1 (d18:1/24:1)
$[M - 2H]^{2-}$	966.44	966.53	GD1, nLD1, and/or LD1 (d18:1/25:0) or (d20:1/23:0)
$[M - 2H]^{2-}$	988.40	988.49	Fuc-GD1 (d18:1/18:2)
$[M - 2H]^{2-}$	990.40	990.51	Fuc-GD1 (d18:1/18:0)
$[M - 2H]^{2-}$	999.41[a)]	999.51	Fuc-GD1 (t18:0/18:0)
$[M - 2H]^{2-}$	1002.41	1002.51	Fuc-GD1 (d18:1/20:2)
$[M - 2H]^{2-}$	1004.42	1004.52	Fuc-GD1 (d18:1/20:0)
$[M - 2H]^{2-}$	1013.44[a)]	1013.53	Fuc-GD1 (t18:0/20:0)
$[M - 2H]^{2-}$	1018.99	1019.02	GalNAc-GD1 (d18:1/18:0)
$[M - 2H]^{2-}$	1032.93[a)]	1033.03	GalNAc-GD1 (d18:1/20:0)
$[M - 3H]^{3-}$	708.39	708.35	GT1 (d18:1/18:0)
$[M - 2H]^{2-}$	1062.96	1063.03	
$[M + Na - 3H]^{2-}$	1073.96	1074.02	
$[M + 2Na - 4H]^{2-}$	1084.93	1085.01	
$[M - 3H]^{3-}$	714.41	714.35	GT1 (t18:0/18:0)
$[M + Na - 3H]^{2-}$	1082.92	1083.02	
$[M - 3H]^{3-}$	717.75	717.69	GT1 (d18:1/20:0)
$[M - 2H]^{2-}$	1076.97	1077.04	
$[M + Na - 3H]^{2-}$	1087.95	1088.03	
$[M + 2Na - 4H]^{2-}$	1098.92	1099.02	
$[M - 3H]^{3-}$	723.75	723.70	GT1 (t18:0/20:0)
$[M + Na - 3H]^{2-}$	1096.93	1097.04	
$[M + Na - 3H]^{2-}$	1094.95[a)]	1095.04	GT1 (d18:1/21:0)
$[M - 3H]^{3-}$	727.11	727.04	GT1 (d18:1/22:0)
$[M + Na - 3H]^{2-}$	1101.92	1102.05	
$[M + Na - 3H]^{2-}$	1108.92[a)]	1109.06	GT1 (d18:1/23:0)
$[M + Na - 3H]^{2-}$	1114.96	1115.06	GT1 (d18:1/24:1)
$[M - 3H]^{3-}$	722.39	722.35	*O*-Ac-GT1 (d18:1/18:0)
$[M - 3H]^{3-}$	731.74	731.70	*O*-Ac-GT1 (d18:1/20:0)
$[M - 2H]^{2-}$	1128.95	1129.05	Fuc-GT1 (d18:1/17:0)
$[M - 2H]^{2-}$	1144.89	1145.06	Fuc-GT1 (t18:0/18:0)
$[M - 2H]^{2-}$	1159.89	1159.08	Fuc-GT1 (t18:0/20:0)
$[M - 3H]^{3-}$	805.40	805.38	GQ1 (d18:1/18:0)
$[M + Na - 4H]^{3-}$	812.73	812.71	
$[M + 2Na - 4H]^{2-}$	1230.43	1230.56	
$[M + 3Na - 5H]^{2-}$	1241.43	1241.55	
$[M - 3H]^{3-}$	814.74	814.72	GQ1 (d18:1/20:0)
$[M + Na - 4H]^{3-}$	822.07	822.05	
$[M + 2Na - 4H]^{2-}$	1244.42	1244.57	
$[M - 3H]^{3-}$	819.38[a)]	819.38	*O*-Ac-GQ1 (d18:1/18:0)
$[M + Na - 4H]^{3-}$	826.73[a)]	826.71	

d = dihydroxy sphingoid base; t = trihydroxy sphingoid base
a) Low intensity ions. Monoisotopic *m/z* values of ions are given.

4 Conclusions and perspectives

Studies upon carbohydrate structure are indispensable to define complex life systems though they were generally considered as extremely difficult because of the lack of the basic efficient technologies commonly used for proteins or nucleic acids. In the past decade, due to the progress in systems biology and ascendant development of specific methods and techniques, glycomics could be introduced as a new concept to follow the genomic and proteomic ones.

MS is crucial for carbohydrate research, by contributing basic understanding of how posttranslational events such as glycosylation affect protein activities. In the past decade, capillary nanoESI-MS has developed as an effective means in glycomics. However, several disadvantages of the method were encountered including low sampling throughput, potential carryovers, and difficult reproducibility due to the variable shape of the spray tip.

The recent introduction of chip-based ESI-MS in glycomics is obviously driven by the higher performance, sensitivity, and reduced analysis time. To date, two different chipESI systems, a thin chip microsprayer and a fully automated chip-based nanoESI robot, have been coupled each to high performance mass spectrometers and tested for structural elucidation of glycoconjugates originating from various biological matrices.

The high sensitivity and ionization efficiency, provided at nano- and microscale level by these systems, will help to establish the new chip-based technology for applications that require identification of unknown, minor components in complex native mixtures of glycoconjugates. Finally, nano- and microchip ESI-MS methods are on the way to become the best suited tools for high-throughput structural elucidation of carbohydrates indicative of pathological states, allowing the chipMS-based glycomics perspectives for large-scale use in biomedical research and clinical diagnostics.

Received February 8, 2005
Revised May 27, 2005
Accepted June 10, 2005

5 References

[1] Dahlin, A. P., Wetterhall, M., Liljegren, G., Bergstrom, S. K., Andren, P., Nyholm, L., Markides, K. E., Bergquist, J., *Analyst* 2005, *130*, 193–199.

[2] Leuthold, L. A., Grivet, C., Allen, M., Baumert, M., Hopfgartner, G., *Rapid Commun. Mass Spectrom.* 2004, *18*, 1995–2000.

[3] Overall, C. M., Tam, E. M., Kappelhoff, R., Connor, A., Ewart, T., Morrison, C. J., Puente, X., *et al.*, *Biol. Chem.* 2004, *385*, 493–504.

[4] Vlahou, A., Schellhammer, P. F., Wright, G. L. Jr., *Adv. Exp. Med. Biol.* 2003, *539*, 47–60.

[5] Sydor, J. R., Scalf, M., Sideris, S., Mao, G. D., Pandey, Y., Tan, M., Mariano, M., *et al.*, *Anal. Chem.* 2003, *75*, 6163–6170.

[6] Huikko, K., Kostiainen, R., Kotiaho, T., *Eur. J. Pharm. Sci.* 2003, *20*, 149–171.

[7] Schultz, G. A., Corso, T. N., Prosser, S. J., Zhang, S., *Anal. Chem.* 2000, *72*, 4058–4063.

[8] Zhang, S., Van Pelt, C. K., Henion, J. D., *Electrophoresis* 2003, *24*, 3620–3632.

[9] Dethy, J. M., Ackermann, B. L., Delatour, C., Henion, J. D., Schultz, G. A., *Anal. Chem.* 2003, *75*, 805–811.

[10] Kapron, J. T., Pace, E., Van Pelt, C. K., Henion, J. D., *Rapid Commun. Mass Spectrom.* 2003, *17*, 2019–2026.

[11] Van Pelt, C. K., Zhang, S., Fung, E., Chu, I. H., Liu, T. T., Li, C., Korfmacher, W. A., Henion, J., *Rapid Commun. Mass Spectrom.* 2003, *17*, 1573–1578.

[12] Xue, Q. F., Dunayevskiy, Y. M., Foret, F., Karger, B. L., *Rapid Commun. Mass Spectrom.* 1997, *11*, 1253–1256.

[13] Ramsey, R. S., Ramsey, J. M., *Anal. Chem.* 1997, *69*, 1174–1178.

[14] Rohner, T. C., Rossier, J. S., Girault, H. H., *Anal. Chem.* 2001, *73*, 5353–5357.

[15] Gobry, V., van Oostrum, J., Martinelli, M., Rohner, T., Rossier, J. S., Girault, H. H., *Proteomics* 2002, *2*, 405–412. Erratum in *Proteomics* 2002, *2*, 1474.

[16] Lion, N., Gellon, J. O., Jensen, H., Girault, H. H., *J. Chromatogr. A* 2003, *1003*, 11–19.

[17] Deng, Y., Henion, J., Li, J., Thibault, P., Wang, C., Harrison, D. J., *Anal. Chem.* 2001, *73*, 639–646.

[18] Dayon, L., Roussel, C., Prudent, M., Lion, N., Girault, H. H., *Electrophoresis* 2005, *26*, 238–247.

[19] Lion, N., Gellon, J. O., Girault, H. H., *Rapid Commun. Mass Spectrom.* 2004, *18*, 1614–1620.

[20] Lion, N., Rohner, T. C., Dayon, L., Arnaud, I. L., Damoc, E., Youhnovski, N., Wu, Z. Y., *et al.*, *Electrophoresis* 2003, *24*, 3533–3562.

[21] Marko-Varga, G., Nilsson, J., Laurell, T., *Electrophoresis* 2003, *24*, 3521–3532.

[22] Williams, J. G., Tomer, K. B., *J. Am. Soc. Mass Spectrom.* 2004, *15*, 1333–1340.

[23] Montreuil, J., Vliegenthart, J. F. G., Schachter, H., *Glycoproteins*, Elsevier, Science B. V. Amsterdam, The Netherlands 1995.

[24] Varki, A., Cummings, R., Esko, J., Freeze, H., Hart, G., Marth, J., *Essentials of Glycobiology*, Cold Spring Harbor Laboratory Press, New York 1999.

[25] Peter-Katalinić, J., *Mass Spectrom. Rev.* 1994, *13*, 77–96.

[26] Zaia, J., *Mass Spectrom. Rev.* 2004, *23*, 161–277.

[27] Zamfir, A., Lion, N., Vukelić, Ž., Bindila, L., Rossier, J., Girault, H. H., Peter-Katalinić, J., *Lab Chip* 2004, 2005, *5*, 298–307.

[28] Bindila, L., Froesch, M., Lion, N., Vukelić, Ž., Rossier, J., Girault, H. H., Peter-Katalinić, J., Zamfir, A., *Rapid Commun. Mass Spectrom.* 2004, *18*, 2913–2920.

[29] Rossier, J. S., Vollet, C., Carnal, A., Lagger, G., Gobry, V., Girault, H. H., Michel, P., Revmond, F., *Lab Chip* 2002, *2*, 145–150.

[30] Rossier, J. S., Youhnovski, N., Lion, N., Damoc, E., Reymond, F., Girault, H. H., Przybylski, M., *Angew. Chem. Int. Ed. Engl.* 2003, *42*, 53–58.

[31] Linden, H. U., Klein, R. A., Egge, H., Peter-Katalinić, J., Dabrowski, J., Schindler, D., *Biol. Chem. Hoppe Seyler* 1989, *370*, 661–672.

[32] Froesch, M., Bindila, L., Zamfir, A., Peter-Katalinić, J., *Rapid Commun. Mass Spectrom.* 2003, *17*, 2822–2832.

[33] Zamfir, A., Peter-Katalinić, J., *Electrophoresis* 2001, *22*, 2448–2457.

[34] Zamfir, A., Peter-Katalinić, J., *Electrophoresis* 2004, *25*, 1949–1963.

[35] Bindila, L., Peter-Katalinić, J., Zamfir, A., *Electrophoresis* 2005, *26*, 1488–1499.

[36] de Jong, J., van den Berg, C., Wijburg, H., Willemsen, R., van Diggelen, O., Schindler, D., Hoevenaars, F., Wevers, R., *J. Pediatr.* 1994, *125*, 385–391.

[37] Sakuraba, H., Matsuzawa, F., Aikawa, S., Doi, H., Kotani, M., Nakada, H., Fukushige, T., Kanzaki, T., *J. Hum. Genet.* 2004, *49*, 1–8.

[38] van Diggelen, O. P., Schindler, D., Kleijer, W. J., Huijmans, J. M. G., Galjaard, H., Linden, H. U., Peter-Katalinić, J., *et al.*, *Lancet* 1987, *2*, 804.

[39] Hakomori, S., *Curr. Opin. Hematol.* 2003, *10*, 16–24.

[40] Nagai, Y., *Behav. Brain Res.* 1995, *66*, 99–104.

[41] Kraćun, I., Rosner, H., Drnovšek, V., Vukelić, Ž., osović, C., Trbojević-Čepe, M., Kubat, M., *Neurochem. Int.* 1992, *20*, 421–431.

[42] Vukelić, Ž., Metelmann, W., Müthing, J., Kos, M., Peter-Katalinić, J., *Biol. Chem.* 2001, *382*, 259–274.

[43] Svennerholm, L., Boström, K., Jungbjer, B., Olsson, L., *J. Neurochem.* 1994, *63*, 1802–1811.

[44] Metelmann, W., Vukelić, Ž., Peter-Katalinić, J., *J. Mass Spectrom.* 2001, *36*, 21–29.

[45] Zamfir, A., Vukelić, Ž., Peter-Katalinić, J., *Electrophoresis* 2002, *23*, 2894–2903.

[46] Vukelić, Ž., Zamfir, A., Bindila, L., Froesch, M., Usuki, S., Yu, R. K., Peter-Katalinić, J., *J. Am. Soc. Mass Spectrom.* 2005, *16*, 571–580.

[47] Zamfir, A., Vakhrushev, S., Sterling, A., Niebel, H. J., Allen, M., Peter-Katalinić, J., *Anal. Chem.* 2004, *76*, 2046–2054.

[48] Zamfir, A., Vukelić, Ž., Bindila, L., Peter-Katalinić, J., Almeida, R., Sterling, A., Allen, M., *J. Am. Soc. Mass. Spectrom.* 2004, *15*, 1649–1657.

[49] Zhang, S., Chelius, D., *J. Biomol. Techn.* 2004, *15*, 120–133.

[50] Froesch, M., Bindila, L., Baykut, G., Allen, M., Peter-Katalinić, J., Zamfir, A., *Rapid Commun. Mass Spectrom.* 2004, *18*, 3084–3092.

[51] Zamfir, A., Seidler, D. G., Kresse, H., Peter-Katalinić, J., *Rapid Commun. Mass Spectrom.* 2002, *16*, 2015–2024. Erratum in *Rapid Commun. Mass Spectrom.* 2003, *17*, 265.

[52] Zamfir, A., Seidler, D. G., Kresse, H., Peter-Katalinić, J., *Glycobiology* 2003, *13*, 733–742.

[53] Zamfir, A., Konig, S., Althoff, J., Peter-Katalinić, J., *J. Chromatogr. A* 2000, *895*, 291–299.

[54] Zamfir, A., Vukelić, Ž., Peter-Katalinić, J., *Electrophoresis* 2002, *23*, 2894 – 2903.

[55] Bindila, L., Almeida, R., Sterling, A., Allen, M., Peter-Katalinić, J., Zamfir, A., *J. Mass Spectrom.* 2004, *39*, 1190–1201.

[56] Vakhrushev, S. Y., Zamfir, A., Peter-Katalinić, J., *J. Am. Soc. Mass Spectrom.* 2004, *15*, 1863–1868.

[57] Mechref, Y., Novotny, M. V., *Chem. Rev.* 2002, *2*, 321–369.

[58] Reinders, J., Lewandrowski, U., Moebius, J., Wagner, Y., Sickmann, A., *Proteomics* 2004, *4*, 3686–3703.

[59] Brooks, S. A., *Mol. Biotechnol.* 2004, *28*, 241–255.

[60] Renfrow, M. B., Cooper, H. J., Tomana, M., Kulhavy, R., Hiki, Y., Toma, K., Emmett, M. R., *et al.*, *J. Biol. Chem.* 2005, *280*, 19136–19145.

[61] Domon, B., Costello, C. E., *Glycoconj. J.* 1988, *5*, 397–409.

[62] Costello, C. E., Juhasz, P., Perreault, H., *Prog. Brain Res.* 1994, *101*, 45–61.

[63] Svennerholm, L., *Adv. Exp. Med. Biol.* 1980, *125*, 11.

[64] IUPAC-IUB Commission on Biochemical Nomenclature, *Eur. J. Biochem.* 1977, *79*, 11–21.

[65] IUPAC-IUB Joint Commission on Biochemical Nomenclature, *Eur. J. Biochem.* 1998, *257*, 293–298.

[66] Roepstorff, P., Fohlman, J., *Biomed. Mass Spectrom.* 1984, *17*, 601–609.

6 Appendix

Ganglioside abbreviations: **LacCer**, Galβ4Glcβ1Cer; **Gg_3Cer**, GalNAcβ4Galβ4Glcβ1Cer; **Gg_4Cer**, Galβ3GalNAcβ4Galβ4Glcβ1Cer; **nLc_4Cer**, Galβ4GlcNAcβ3Galβ4Glcβ1Cer; **GD3**, II_3-α-$(Neu5Ac)_2$-LacCer; **GT3**, II^3-α-$(Neu5Ac)_3$-LacCer; **GM2**, II^3-α-Neu5Ac-Gg_3Cer; **GD2**, II^3-α-$(Neu5Ac)_2$-Gg_3Cer; **GM1a**, II^3-α-Neu5Ac-Gg_4Cer; **GM1b**, IV^3-α-Neu5Ac-Gg_4Cer; **GD1a**, IV^3-α-Neu5Ac,II^3-α-Neu5Ac-Gg_4Cer; **GD1b**, II^3-α-$(Neu5Ac)_2$-Gg_4Cer; **GT1b**, IV^3-α-Neu5Ac,II^3-α-$(Neu5Ac)_2$-Gg_4Cer; **GQ1b**, IV^3-α-$(Neu5Ac)_2$,II^3-α-$(Neu5Ac)_2$-Gg_4Cer; **3'-nLM1 or nLM1**, IV^3-α-Neu5Ac-nLc_4Cer; **nLD1**, disialo-nLc_4Cer (IV^3-α-$(Neu5Ac)_2$-nLc_4Cer